

NASA Technical Memorandum 81166

(NASA-TM-81166) OBJECTIVE MEASUREMENT OF
HUMAN TOLERANCE TO +G SUB Z ACCELERATION
STRESS Ph.D. Thesis - Univ. of N. Indiana
(NASA) 100 p HC A05/MF A01

N80-18709

CSCL 06S

Unclas
G3/52 47250

Objective Measurement of Human Tolerance to +G_z Acceleration Stress

Salvadore A. Rositano

February 1980



NASA

National Aeronautics and
Space Administration

Objective Measurement of Human Tolerance to $+G_z$ Acceleration Stress

Salvadore A. Rositano, Ames Research Center, Moffett Field, California



National Aeronautics and
Space Administration

Ames Research Center
Moffett Field, California 94035

TABLE OF CONTENTS

<u>Section</u>	<u>Title</u>	<u>Page No.</u>
	Table of Contents-----	iii
	List of Illustrations-----	vi
1.0	INTRODUCTION-----	1
2.0	NATURE OF ACCELERATION-----	5
3.0	PHYSIOLOGY OF +Gz ACCELERATION-----	7
3.1	Cardiovascular Effects-----	7
3.2	Visual Effects-----	11
4.0	OBJECTIVE AND SUBJECTIVE END POINTS IN +Gz RESEARCH-----	13
4.1	Subjective Visual End Points-----	13
4.1.1	Limitations-----	13
4.2	Objective End Points-----	15
4.2.1	Eye Level Blood Pressure-----	15
4.2.2	Retinal Artery Observation-----	16
4.2.3	Electroencephalogram (EEG)-----	16
4.2.4	Electrocardiogram (ECG)-----	17
4.2.5	Ear Opacity-----	17
5.0	INSTRUMENTATION METHODS-----	19
5.1	Doppler Ultrasonic Flowmeter-----	19
5.1.1	Basic Description of Doppler Flowmeters-----	20
5.1.2	Non-Directional Flowmeter Theory-----	20

PRECEDING PAGE BLANK NOT FILMED

5.1.3	Directional Flowmeter Theory-----	22
5.1.4	Doppler Audio-----	30
5.1.5	Transducer Development-----	30
5.1.6	Probe Attachment Over the Temporal Artery-----	33
5.2	Centrifuge Facilities-----	35
5.3	Subject Safety-----	35
5.4	Conventional Visual End Point Apparatus-----	40
5.5	Data Acquisition-----	41
6.0	EXPERIMENTAL METHODS-----	42
6.1	Preliminary Test at Ames Research Center-----	42
6.1.1	Results-----	43
6.2	Methods for Correlating Temporal Flow Velocity and Direct Eye Level Blood Pressure-----	46
6.2.1	Results - Diastolic Reverse Flow Hypothesis---	48
6.2.2	ROR Results-----	48
6.2.3	GOR Results-----	50
6.3	Critical Evaluation of GOR End Point and Temporal Blood Flow-----	54
6.3.1	Results-----	55
6.4	Correlation of Temporal Artery and Common Carotid Artery Flow During +Gz-----	55
6.4.1	Results-----	57
6.5	Correlation of Temporal Artery Flow and Objective Visual Field Limit-----	59
6.5.1	ROR Results-----	61
6.5.2	GOR Results-----	63
6.5.3	GOG Results-----	66
6.6	Applications to G Protection Technique Evaluation-----	66
6.6.1	Results - Straining Maneuvers-----	68
6.6.2	Results - G-Suit-----	70

6.6.3	Results - Tilt Back Seat-----	72
6.7	Safety-----	74
7.0	DISCUSSION-----	82
7.1	Correlation With Direct Eye Level Blood Pressure-----	82
7.2	Correlation With Visual End Points-----	85
7.3	Comparison to Ear Opacity End Points-----	86
7.4	Limitations-----	87
8.0	CONCLUSIONS-----	88
9.0	REFERENCES-----	89
	VITAE-----	93

LIST OF ILLUSTRATIONS

Figure No.	Title	Page No.
------------	-------	----------

TABLES:

I	Relationship Between Stages of Visual Symptoms and Vascular Changes in the Fundus of the Eye-----	12
---	---	----

FIGURES:

1.	Factors Affecting Visual Function-----	3
2.	Hydrostatic Pressures at G-----	9
3.	Basic Doppler Flowmeter Block Diagram-----	23
4.	Directional and Non Directional Flow-----	24
5.	Ames 6CH Wireless Telemetry Doppler-----	25
6.	Ames 3CH Hardwire Telemetry Doppler-----	26
7.	Ames 4CH Directional Doppler for Lab Use-----	28
8.	Ames 2CH Directional Doppler Flowmeter-----	29
9.	Variable Angle Doppler Probes-----	31
10.	Typical Transcutaneous Probes-----	32
11.	Locating Maximum Temporal Artery Pulse-----	34
12.	Affixing Sensors to Skin-----	34
13.	Doppler Sensors in Place Over Temporal Artery-----	34
14.	20 G Centrifuge NASA-Ames-----	36
15.	Human Centrifuge USAF SAM-----	37
16.	Subject Seating - NASA-Ames-----	38
17.	Subject Seating - USAF SAM-----	39
18.	Radial and Temporal Artery Flow - GOR-----	44
19.	Harness for Eye Level Pressure Cell-----	47
20.	Retrograde Diastolic Flow Confirmed-----	49
21.	Eye Level Blood Flow and Pressure - ROR-----	51
22.	Latency of Visual Response - ROR-----	52

LIST OF ILLUSTRATIONS

<u>Figure No.</u>	<u>Title</u>	<u>Page No.</u>
23.	Negative Mean Blood Flow as End Point-GOR-----	53
24.	Subjective and Objective End Points-GOR-----	56
25.	Carotid and Temporal Blood Flow Compared-ROR-----	58
26.	Gillingham Light Bar - USAF SAM-----	60
27.	Blood Flow, Pressure and Visual Response to ROR---	62
28.	Compensatory Response During ROR-----	64
29.	Blood Flow Pressure and Visual Response-GOR-----	65
30.	Blood Flow, Pressure and Visual Response-GOG-----	67
31.	Response to "L-1" Maneuver During ROR-----	69
32.	g-Suit Inflation Modifies Eye Level Blood Flow----	71
33.	Relaxed, g-Suit, Valsalva Comparison-----	73
34.	Response to 13° Tilt Back Seat-----	75
35.	Response to 45° Tilt Back Seat-----	76
36.	Response to 65° Tilt Back Seat-----	77
37.	Pulsus Alternans During ROR-----	79
38.	Pulsus Alternans During GOR-----	80
39.	Pulsus Alternans During G on G-----	81
40.	Proximity of Temporal and Ophthalmic Arteries-----	84

OBJECTIVE MEASUREMENT OF HUMAN TOLERANCE TO $+G_z$
ACCELERATION STRESS

Salvadore A. Rositano
Ames Research Center

1.0 INTRODUCTION

Outside of the problems associated with reduced barometric pressure, there is no field in the whole of aerospace bioscience that has received so much attention as acceleration. As our space exploration efforts extend opportunities for manned flight to passengers with various degrees of physical fitness accurate assessment of tolerance to acceleration is imperative. Flight experience and weightlessness simulation experiments have shown evidence of cardiovascular deconditioning after periods of sustained weightlessness (Leverett, 1971 and Greenleaf, 1973). Atmospheric reentry after a long stay at weightlessness may very well be the most critical time in the space mission.

The Space Shuttle orbiter will reenter and land in a manner that may impose a head-to-foot acceleration vector upon crew and passengers seated in normal upright position. Reentry from the long Skylab missions did not produce intolerable G loads on the crew; however, the inclusion of non-astronaut scientific personnel and subjection of passengers (not necessarily young, physically fit males) to positive acceleration loads requires an extensive evaluation of the physiological effects of weightlessness and subsequent acceleration tolerance.

A major obstacle in $+G_z$ research, in which the inertial vector acts in a head-to-foot direction, is the lack of reliable techniques for objective measurement of cardiovascular status. Acceleration

stress is generally evaluated by use of a man-carrying centrifuge by creating an increased gravitational field and recording the elapsed time to subjective visual field degradation. Motivation, experience, and several uncontrollable factors seem to affect the subject's response to changes in vision as tolerance limit is approached. In the presence of high onset rate (≥ 1 g/sec) a subject may become unconscious with little or no prior warning. To accurately predict tolerance to positive acceleration a rapid-response-time objective analysis of physiological functions must be used.

Reduced oxygen levels in cerebral blood supply has been found empirically to be associated with loss of visual function - first as greyout (loss of peripheral vision); then blackout (loss of vision), and finally unconsciousness. Unfortunately, loss of vision is a continuum from loss of peripheral vision through to unconsciousness.

Factors which effect changes in vision are not simple as may be seen in Figure 1. Availability of oxygen and glucose in the cerebral blood supply is essential to maintenance of visual function. Basic properties affecting delivery of blood are, of course, cerebral blood flow, F ; arterial pressure, P ; and vessel resistance, R_z ; as related in the equation:

$$F = P/R_z$$

In the presence of acceleration R_z remains constant or decreases;

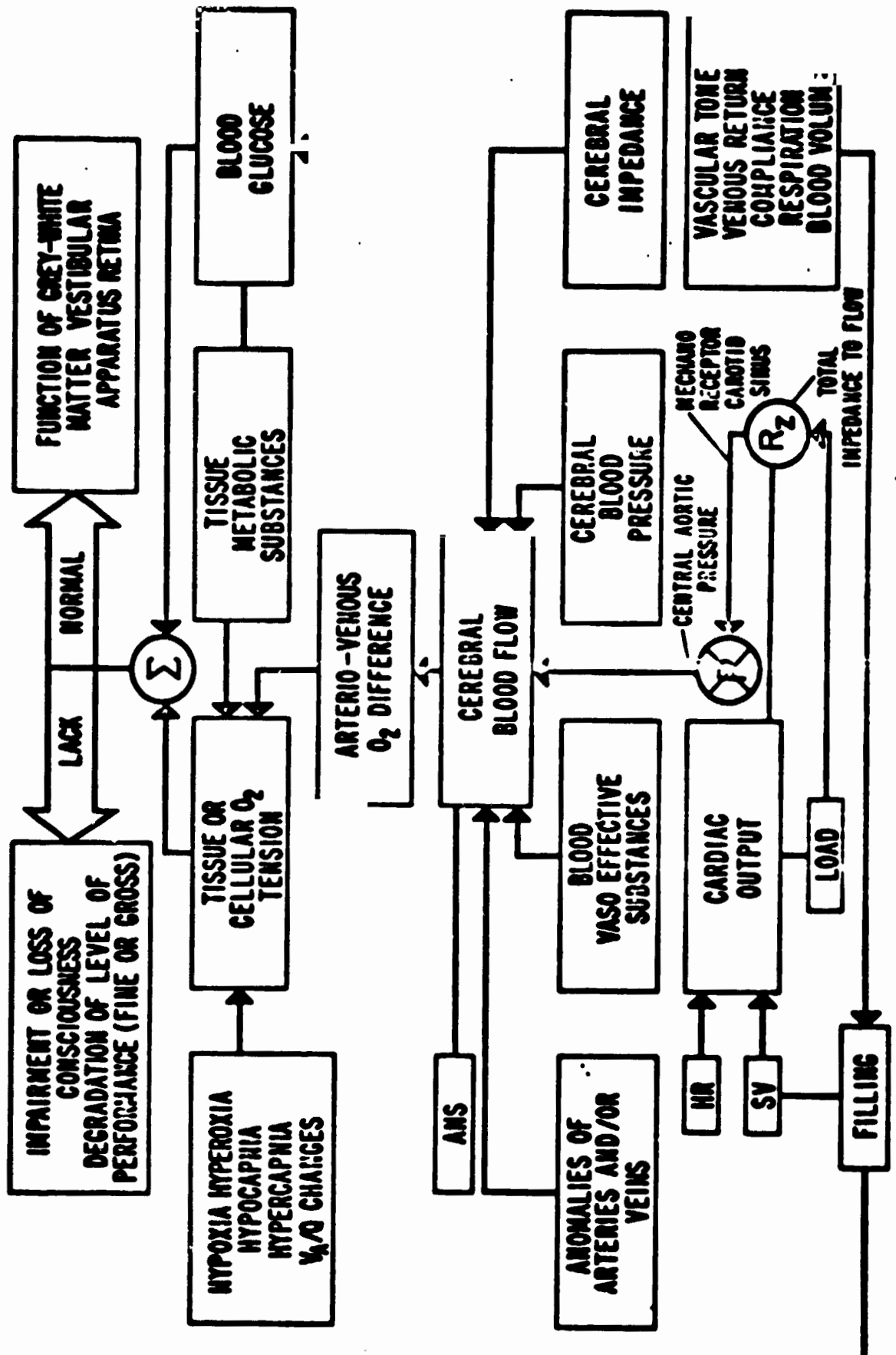


Figure 1. Factors which affect vision.

therefore, a reduction in oxygen delivery, leading to visual impairment, may be effected by reduced flow or pressure. Data in this study will confirm the relationship between visual degradation and reduced pressure and flow. Until the developments reported here only direct, invasive, head level blood pressure was considered as an objective indicator of cerebral blood supply. Instead of using vision as a subjective indication of reduced O_2 level, due to decreased flow, i.e. decreased pressure, flow will be used directly.

This thesis describes a noninvasive method for monitoring the acceleration-stressed human subject by measurement of temporal artery blood flow velocity using a transcutaneous Doppler ultrasonic flowmeter. Correlation will be made with direct eye level blood pressure as well as subjective visual symptoms in the presence of several types of acceleration profiles. The study will be limited to evaluating the feasibility, reliability, and applications of the new method to only the most critical, head-to-foot acceleration vector.

2.0 NATURE OF ACCELERATION

By definition, acceleration is a rate of change, and it can occur in any or all of three related, but differing maneuvers. Linear acceleration is the rate of change of velocity of mass, the direction of movement of which is kept constant. Angular acceleration is the rate of change of direction of mass, the velocity of which is kept constant. In this regard, the acceleration is directly proportional to the square of the velocity and inversely proportional to the radius of turn. By common usage, where the axis of rotation is external to the body, as in an aircraft turn or a centrifuge, the acceleration is frequently termed "radial" acceleration, while the term "angular" is better retained for situations where the axis of rotation passes through the body. In its third form, acceleration occurs as a component of the attraction between masses. Newton showed that the force of attraction between masses is directly proportional to the product of the masses and indirectly proportional to the square of the distances between them, and that the proportionality constant is the gravitational constant g , which represents an acceleration of 32.24 feet per second when earth gravitation is a component of the system.

The term "G" used in this text is used to indicate the inertial resultant of body acceleration, not the acceleration itself. It thus represents the resultant of vehicular displacement acceleration and gravitational acceleration, and is measured in gravitational units.

Positive and negative signs are used to delineate the vector. By convention $+G_z$ indicates that the heart is displaced toward the feet; $-G_z$ indicates that the heart is displaced toward the head. Similarly, $+G_x$ indicates displacement of the heart toward the back, and $-G_x$ indicates displacement of the heart toward the sternum. Again by convention, $+G_y$ and $-G_y$ indicates displacement of the heart to the left and right, respectively.

The terms used in describing the duration of acceleration should also be defined. Three duration classes are generally used; "Abrupt Acceleration" has a duration of 0.2 seconds or less; "brief acceleration" extends to 10 seconds; "prolonged acceleration" refers to durations longer than 10 seconds. For purposes of this paper "sustained acceleration" will be used to describe either brief or prolonged acceleration (Fraser, 1966).

Rate of onset affects human tolerance as will be described later. Rapid onset (ROR) refers to acceleration profiles which exceed 0.5 g/sec, while gradual onset (GOR) describes a rate of onset which is less than 0.5 g/sec. "GOG" (G on G) describes a variable acceleration profile, such as an evasive maneuver of a fighter aircraft.

3.0 PHYSIOLOGY OF +G_Z ACCELERATION

The physiological changes found in acceleration are fundamentally related to the increase in weight and hydrostatic pressure that develops along a vector of the acceleration. Thus, the effects vary according to the position of the body with respect to the vector. When applied in the +G_Z vector the limiting effects are primarily cardiovascular; when applied in the +G_X or +G_Y, however, they are primarily respiratory. As previously stated, only +G_Z is treated in this paper due to its operational importance for space and military applications.

In the centrifuge control room at the USAF School of Aerospace Medicine hangs an appropriate plaque containing names of subjects who have successfully passed a high +G_Z test. The coat of arms of this certificate and all gravitational physiologists is the giraffe, for man is functionally converted to giraffe as increased +G_Z acceleration increases the head to heart hydrostatic pressures as shown in Figure 2 and discussed in the material to follow.

3.1 Cardiovascular Effects

Pascal, in the 17th century, showed that in ideal fluids at rest, (a) fluid pressure exerted at any point in a confined liquid is transmitted undiminished in all directions, (b) pressures at points lying in the same horizontal plane are equal, and (c) pressure increases with depth under the free surface. This increase

is equal to ρgh dynes/cm², where ρ is the density of the fluid, g the gravitational constant, and h the depth. These laws apply to the vascular system, and after a fashion, to the body as a whole. Thus a mean arterial pressure at heart level of 100 mmHg will support a column of blood 130 cm high (Burton, 1960) and the mean arterial pressure at feet and brain are approximately the same when the body is horizontal. When the body is erect, the effect of change in weight is such as to decrease mean arterial pressure in the brain and increase it in the feet. In the erect position a brain-to-heart column of blood 250 mm high produces $250 \text{ mm} \div 13 \text{ mm/mmHg}$, or 19 mmHg back pressure on the heart. Thus, a mean arterial pressure of 100 mmHg at heart level becomes 100-19 or 81 mmHg at brain level. Similarly arterial pressure in the feet will become approximately 175 mmHg.

Under increased acceleration, the resultant between applied and gravitational acceleration acts to increase the effective density of the blood, i.e. increases the g component in the ρgh equation according to the magnitude of the g units of the applied acceleration. This is illustrated in Figure 1 (Wood, et al, 1963), which is a diagrammatic representation of hydrostatic pressures in the vascular system of a man sitting in the upright position at 1 G and under exposure to +5 G_z. The center sketch, illustrating the vascular effects at 1 G indicates that with a mean arterial pressure of 120 mmHg the mean pressures at head and foot levels

**BLOOD PRESSURE (B.P.) AT ANY LEVEL
EQUALS HEART LEVEL PRESSURE (Pa)
PLUS HYDROSTATIC PRESSURE (Ph)**

$$B.P. = Pa + P_h$$

$$Pa = 120 \text{ mmHg}$$

$$Ph = 5 \times 24 = 120 \text{ mmHg}$$

$$B.P. = 120 - 120 = 0 \text{ mmHg}$$

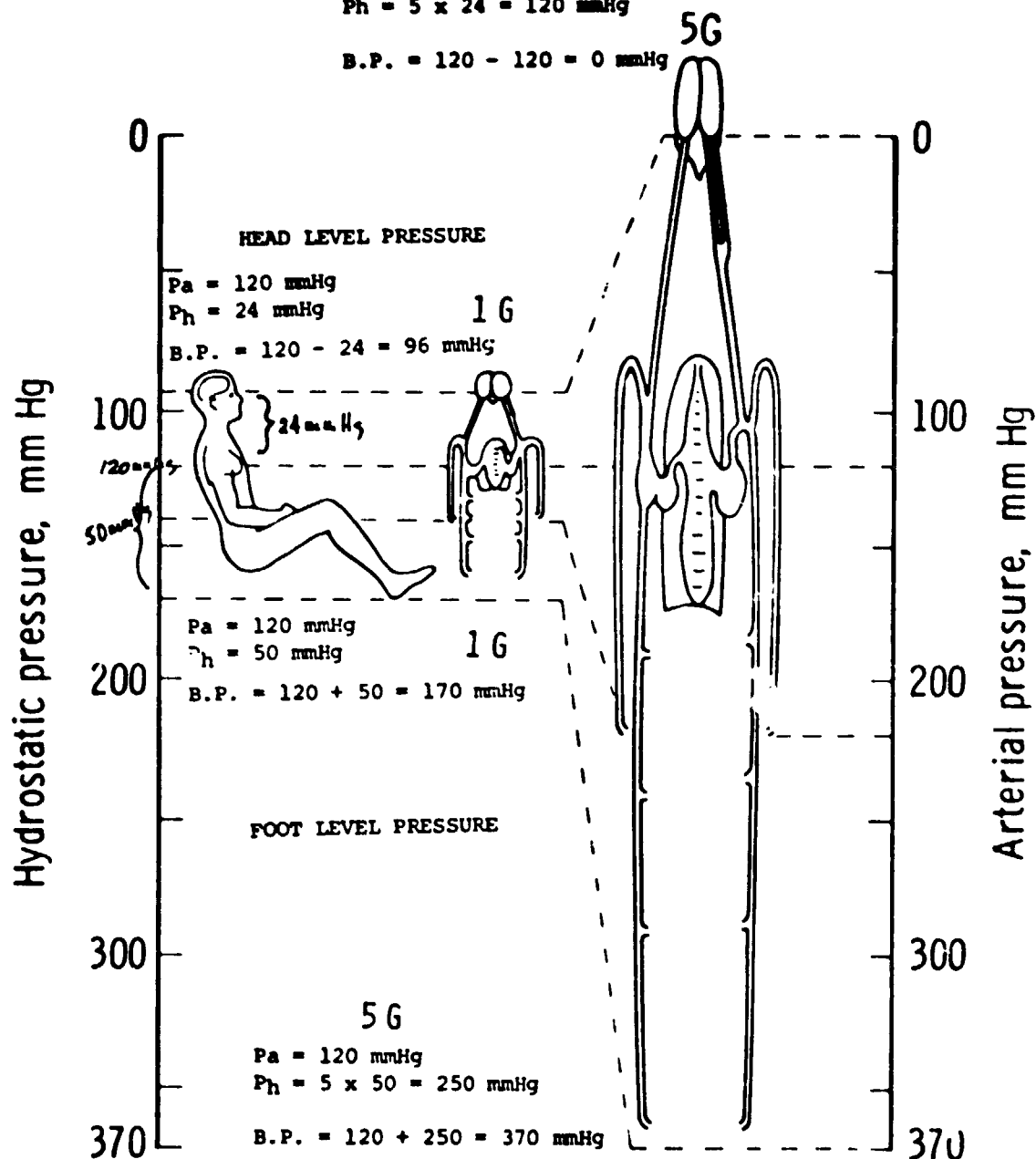


Figure 2. Diagrammatic representation of hydrostatic pressures in vascular system of a man in upright sitting position at 1G and during headward acceleration at 5G. (Wood et al. 1963)

are calculated to be 96 and 170 mmHg respectively. At +5 G_z, while maintaining mean arterial pressure at heart level of 120 mm Hg, the calculated pressure at the base of the brain will be zero, while at the feet it will be 370 mmHg. Under these circumstances the subject would be unconscious and an additional venous pressure of 250 mmHg would be required to return blood from feet to heart. Fortunately, unconsciousness does not necessarily occur at +5 G_z, since compensatory adjustments occur on the cardiovascular system. The foregoing hydrostatic explanation is important because initial blood pressure response to +G_z follows the hydrostatic model. Lambert and Wood (1946) showed by progressive exposure of subjects to increased magnitude of acceleration that the fall in blood pressure at head level was proportional to the magnitude of acceleration. The blood pressure at heart level, however, is maintained near normal, or in fact, may actually increase to hypertensive levels at 5 G because of vasoconstrictive compensatory measures.

Further correlation of blood pressure changes with other parameters are recorded by Lindberg and Wood (1963), who point out that during acceleration with rates of onset from 1 to 2 G per second, which are of magnitudes sufficient to produce loss of vision there is an immediate decrease in blood pressure at head level, an increase in heart rate, a decrease in blood content of the ear, and a decrease in the amplitude of the arterial pulse at

the level of the ear. This leads in turn to failure of peripheral vision and eventually of central vision.

Direct measurement of eye level blood pressure is considered to be the most accurate objective indicator of $+G_z$ tolerance. The noninvasive technique suggested in this thesis has been extensively compared with direct eye level arterial pressure and receives much of its credibility from demonstrated relationship to arterial pressure change during $+G_z$.

3.2 Visual Effects

Reduction in blood supply to the head area because of decreased blood pressure has been closely correlated with diminished visual field and eventually unconsciousness.

Andina (1937) became interested in the problem of the "black veil" which was experienced during the pullout from a dive "just at the moment when the shot should be fired." His laboratory work as well as experiments in an airplane provided by the Swiss Air Force produced the salient observation of the importance of the difference in pressure between the retinal artery and intraocular pressure. Andina proposed that the blood pressure in the retinal artery must be greater than the intraocular pressure before any blood will flow in the eye.

Lambert (1945) with Wood (1946) provided the first experimental evidence on the role of the retina in the origin of blackout.

Duane (1954) using direct ophthalmoscopic observations, and Leverett and Newsom (1971) using retinal photography and fluorescence angiography, found that subjective blackout coincides with cessation of flow in the retinal circulation. Leverett and Newsom also found that visual failure at blackout occurred when head level mean arterial pressure had fallen below 20 mmHg. In a later paper, Duane, et al (1962) showed that where the hydrostatic pressure was such as to cause collapse of the arteriolar vessels during diastole and recovery in systole, a pulsation of the vessels may be observed which is associated with grayout, or reduction of the visual field to approximately 15° in all meridians.

Duane's observations are summarized in Table I below. Time lags of two to five seconds were reported between the ophthalmoscopic findings and the subjective effects. This observation as well as the classic color fundus photographs obtained by Leverett will be important basis for establishing the validity of the noninvasive technique to be presented in this thesis.

Table I - Relationship Between Stages of Visual Symptoms and Vascular Changes in the Fundus of the Eye

<u>Stage</u>	<u>Subjective</u>	<u>Objective</u>
I	Loss of peripheral lights	Arteriolar pulsation
II	Blackout	Arteriolar exsanguination and collapse
III	Return of central and peripheral lights	Return of arteriolar pulsation and temporary venous distension

4.0 OBJECTIVE AND SUBJECTIVE END POINTS IN +G_z RESEARCH

4.1 Subjective Visual End Points

Increased speed and performance of modern aircraft as well as space flight reentry conditions make the problem of human tolerance and reaction to acceleration more complex. However, the cardiovascular effects leading to blackout and unconsciousness tend to remain the same if the G level is above the control blackout level of the subject. Since the pattern of blackout and unconsciousness is essentially the same in all subjects, objective end points for human tolerance would seem possible; however, several factors make the end point for any given subject somewhat subjective.

4.1.1 Limitations

Objective measurement techniques relieve the subject of responsibility of trying to make a rational assessment of his own physiological state. In addition, it does not readily lend itself to falsification, especially by an unmotivated or anxious subject. Chambers (1963) summarized several variables which complicate human tolerance determination. Some of his observations included:

- (a) Emotional factors such as fear and anxiety, confidence in self and apparatus, and willingness to tolerate discomfort and pain.
- (b) Motivational factors such as competitive attitude, desire to be selected for a particular space project, or specific pay, recognitions or awards.

- (c) Previous acceleration training and accumulative effects.
- (d) Presence or absence of performance tasks which must be done during peak G stress.
- (e) Body positions, protective devices, breathing techniques, etc.
- (f) Age of subject.
- (g) Types of end points used.

The classical end points used in human acceleration experiments are the visual end points of loss of peripheral vision (gray-out) and loss of all vision (blackout).

Coburn (1970) voiced his concern regarding the "reliability and repeatability of a large portion of the data reported in the literature." Many of his objections to subjective end points have been verified by other acceleration physiologists. An inexperienced centrifuge subject may terminate a run because of fear or a misunderstanding of the desired end point. Even an experienced, highly motivated subject will terminate a run prematurely if unduly fatigued by previous runs. Even more important is the danger that some individuals will progress to unconsciousness during rapid onset acceleration without recognizing a gradual deterioration of vision. Visual end points are useful as Coburn points out, for highly trained, motivated subjects.

Regardless of motivational/emotional state of the subject, the spatial and temporal characteristics of the light sources used in

the visual end point method are very important. For any given set of visual stimuli the problem of what constitutes the phenomena known as grayout and blackout becomes even more difficult for inexperienced subjects. The medical monitor usually describes each end point and then lets the subject decide for himself when he has reached it. This seems straightforward; however, subjects, even experienced ones, will describe their experiences differently.

Most centrifuges use a fixed set of three colored lamps arranged on a linear, horizontal bar at a fixed distance from the eyes. A center red light is used as fixation point and the criterion for central vision loss (blackout) is when intensity dims considerably or disappears. Peripheral light loss is established by disappearance of flashing green lights placed at 15°-25° each side of the center red light.

This author has witnessed several tests where the subject has reported full loss of the central red light while still sensing the flashing peripheral green lights. Subjects may report a color change from green to white in this instance, however, blackout followed by unconsciousness was eminent.

4.2 Objective End Points

4.2.1 Eye Level Blood Pressure

The works of Lambert, Wood, Leverett and others previously cited certainly provide techniques for establishing conclusive

repeatable cardiovascular end points. Radial arterial cannulation with the blood pressure referenced at eye level has remained the objective $+G_z$ tolerance measurement choice since the pioneering work of Lambert and Wood (1946) in correlating eye level blood pressure and visual symptoms. This is due to the fact that neither flow or resistance could be measured invasively, or noninvasively. Direct cannulation of the radial artery requires inherent risks, discomfort, and possible influence on acceleration tolerance (Ryan, 1973; Samaan, 1971).

4.2.2 Retinal Artery Observation

Direct observations of retinal arterial blood flow would also provide excellent determination of objective end points; however, the method is extremely difficult to implement, costly and impractical at high G levels.

4.2.3 Electroencephalogram (EEG)

EEG measurements have been correlated with changes in visual fields. Sem-Jacobsen (1958-1961) found marked changes in EEG in pilots undergoing violent flying maneuvers. Squires, et al (1964) reported EEG changes in subjects during blackout produced by $+G_z$ acceleration. Frequency analysis showed characteristic changes during grayout and blackout. An increase in beta frequencies (16 to 36 Hz) occurred and the general amplitude pattern was coincident with the acceleration profile. Other frequency changes were reported during grayout and blackout; however, the authors considered

that the best index of consciousness appeared to be in an inverse relationship between amplitude of components in the 5 cps range and the depth of blackout. Difficulty of applying the technique has made consistent interpretation a matter of conjecture. Muscle problems, muscle artifacts, variations of subject response are but a few of the problems (Coburn, 1970).

4.2.4 Electrocardiogram (EKG)

Clinical analysis of EKG is always used as a medical safety procedure. Fraser (1966) reports little conclusive evidence of end point criteria from EKG recordings. Several anomalies may appear during and after acceleration stress but none can be consistently associated with impending visual failure (Brown and Fitzimmons, 1957). Although increased pulse rate almost always accompanies G stress, no end point criteria can be determined. Pulse rate is useful, however, in comparing performance of several subjects or as comparative data before and after altering the subject's environment or physical conditioning, such as weightlessness.

4.2.5 Ear Opacity

Wood, et al (1963) describe a technique whereby the blood content present in the pinna of the ear is estimated by means of a light source/photosensor configured to record transmissibility. Increase in ear opacity has been correlated with decline in blood pressure at increased G_z . McGuire, et al (1961) and Smedal, et al (1963) report qualitative changes in ear pulse and opacity with

various acceleration profiles. Disappearance of the ear pulse has been used by these groups as an indication of impending visual failure. Wood, et al (1963) used relative changes in ear opacity to measure G protection afforded by water immersion. This group reported excellent correlation between systolic arterial pressure and amplitude of ear opacity pulse at levels of headward acceleration high enough to reduce diastolic arterial pressure at head level to zero. They further suggested that the use of ear opacity pulse was a good analog for judging decreased systolic pressure at head level. No other reports on use of this technique as an end point criterion could be found.

5.0 INSTRUMENTATION METHODS

Special instrumentation for use at high G was developed for this study. Principles of centrifuge and noninvasive blood flow instrumentation will be reviewed. Two types of Doppler flowmeters were utilized. Both measured flow velocity magnitude; however, one was non-direction-sensitive, while the other was capable of also measuring direction.

5.1 Doppler Ultrasonic Flowmeter

The use of the Doppler principle in cardiology was first suggested by Satomura (1957, 1959, 1960). Practical application of the principle with an analog readout began with the work at the University of Washington under Dr. R. F. Rushmer and D. L. Franklin (1961). Flowmeter electronics used until 1967 could not distinguish flow direction; however, F. D. McLeod (1967, 1969) published the first results using a direction-sensitive flowmeter. Flowmeters of the Franklin and McLeod types as modified by Rositano, et al (1969, 1973) were used in this study.

Transducers specifically designed for non-invasive transcutaneous use were introduced by Rushmer (1966) and Stegal (1966). Specific transducers were designed to meet the needs of this study by Mancini and Rositano (1973).

5.1.1 Basic Description of Doppler Flowmeters

The change of pitch in a railroad whistle as it passes a stationary observer is caused by the Doppler effect. If a continuous beam of ultrasound is transmitted diagonally into a column of blood, a small fraction of the sound energy backscatters from the particles in the blood to reach a receiver located adjacent to the transmitter. If the blood is stationary, the ultrasonic frequency at the receiver is the same as the transmitter frequency. If the blood is moving, however, a Doppler shift in frequency occurs such that the ultrasound reaching the receiver differs from the transmitted frequency by the amount dependent, in part, upon the velocity with which the backscattering particles are moving. By mixing the transmitted frequency with the backscattered frequency a beat frequency is generated which is audible (0 to 10000 Hz) under normal blood flow conditions and can be recorded to indicate dynamic changes in blood flow velocity in arteries and veins. The following development more specifically details the continuous wave Doppler flowmeter theory.

5.1.2 The Non-Directional Flowmeter

Blood cells provide sufficient interface to scatter and reflect a small portion of an incident beam of high frequency (5-11 MHz) ultrasound. The frequency of waves scattered from stationary

interfaces is the same as that of the incident wave; however, waves scattered from moving particles experience a frequency shift proportional to the scattering cell's velocity. The frequency shift, described by the Doppler equation is:

$$F_d = \frac{2F_c V_i \cos \alpha}{C}$$

where F_d = frequency shift or difference frequency,

F_c = frequency of incident wave,

V_i = vector component of scattering particles velocity along an axis bisecting the angle between the transducer elements,

α = half angle between transducer elements and flow axis,

C = velocity of sound in fluid.

For a typical physiological application: $F_c = 10$ MHz; $C = 1.4 \times 10^3$ M/sec; $\alpha = 45^\circ$; V ranges from 0 to ± 1 m/sec; the Doppler shift ranges from 0 to 10 kHz.

The blood stream consists of a large number of random scatters moving in a velocity profile. The scattered signal is not a discrete frequency but a power spectrum representative of the flow profile (McLeod, 1969). The reflected signal is expressed as

$$P(F_d) = A(V)$$

where $A(V)$ is the vessel crosssectional area occupied by fluid moving at velocity V and illuminated by the ultrasonic beam. The large number of random on Gaussian scatters permits expression of the mean velocity as the first moment of the power spectrum $[P(F_d)]$.

The power received at the second or receiving piezoelectric transducer is amplified and demodulated so as to preserve both amplitude and phase information. The demodulation process shown in Figure 3 translates the scattered power spectrum to the origin where the direct coupled carrier appears as a zero frequency of DC component and is easily removed with a blocking capacitor. A zero crossing detector is used to produce a voltage output proportional to the mean flow velocity. Although errors due to non-uniform Doppler spectra, have been noted in its use by Flax, et al (1970) and others, the zero crossing detector performs satisfactorily for this study. Absolute magnitude of flow will not be used. Relative changes in velocity and, more importantly, flow direction and the presence or absence of flow signals will be used exclusively.

Since only F_d , the difference frequency, is detected and since its algebraic sign is unknown, movement away from the crystals at velocity V results in the same output from the zero crossing circuit as movement toward the crystals at this velocity, as shown in Figure 4.

Non-directional systems developed for centrifuge use at NASA-Ames Research Center are shown in Figures 5 and 6.

5.1.3 Directional Flowmeter

In a device developed by McLeod (1967) a phase shift is introduced prior to detection, making possible the identification and

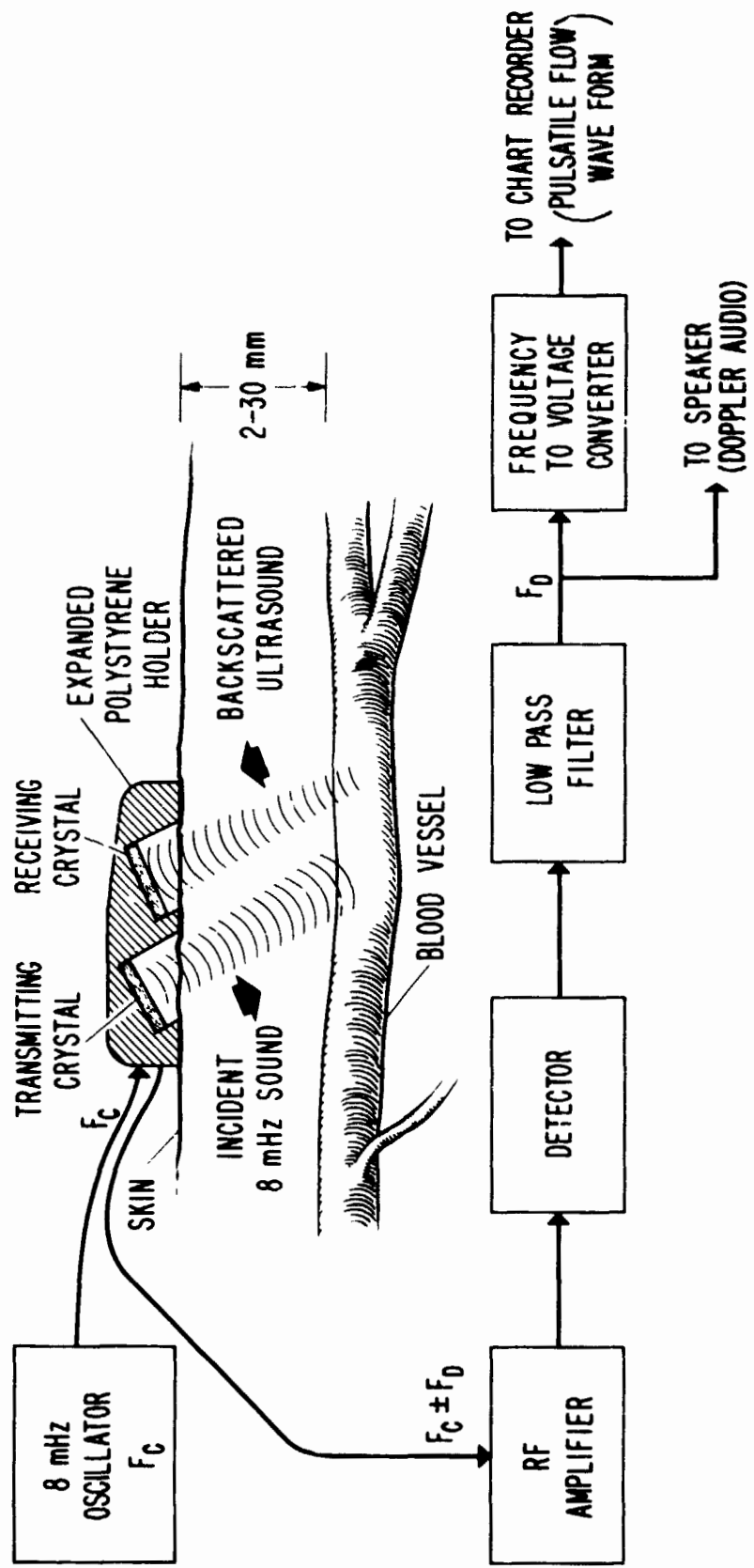
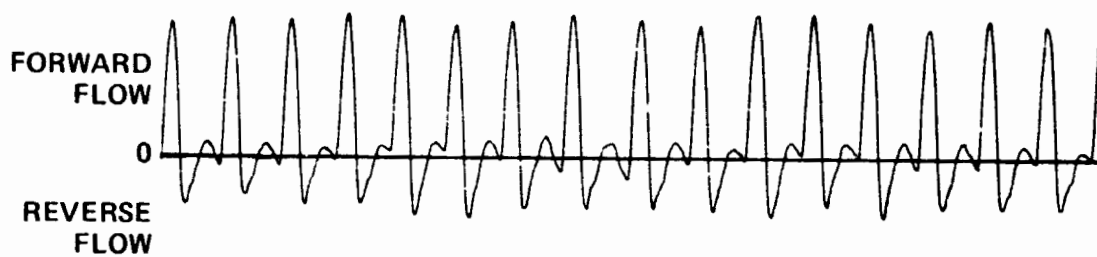
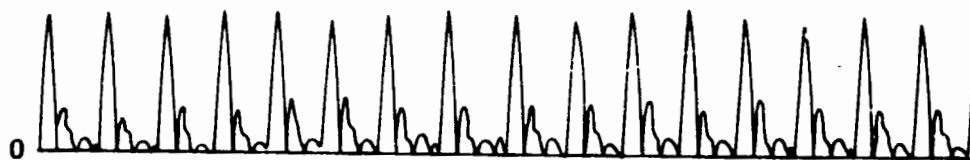


Figure 3. Block diagram of non-directional Doppler ultrasonic flowmeter



DIRECTION SENSITIVE DOPPLER WAVEFORM



NON-DIRECTIONAL DOPPLER WAVEFORM

Figure 4. Comparison of waveforms from non-direction sensitive and directional Doppler flowmeters

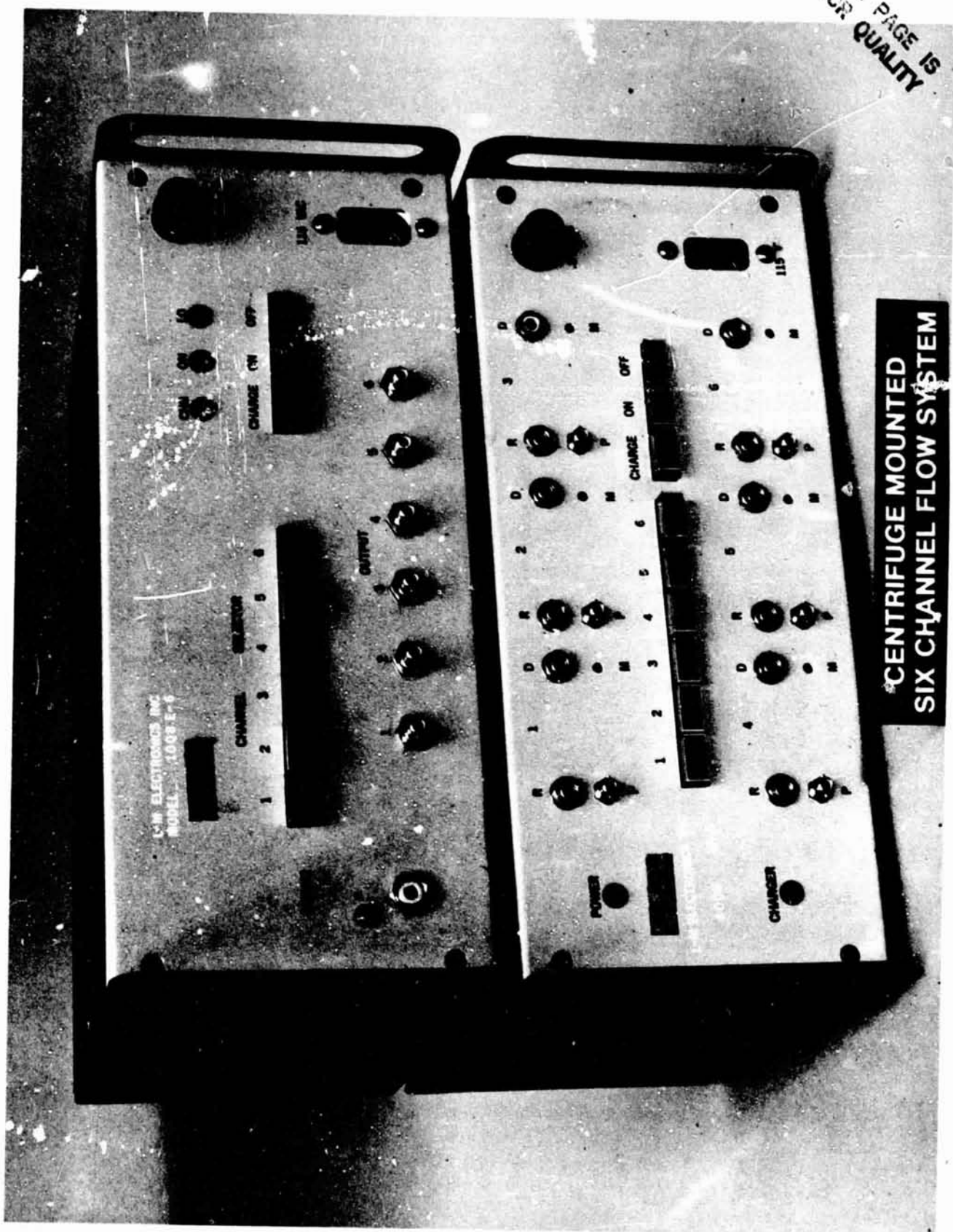


Figure 5. Ames six channel wireless telemetry Doppler flowmeter.

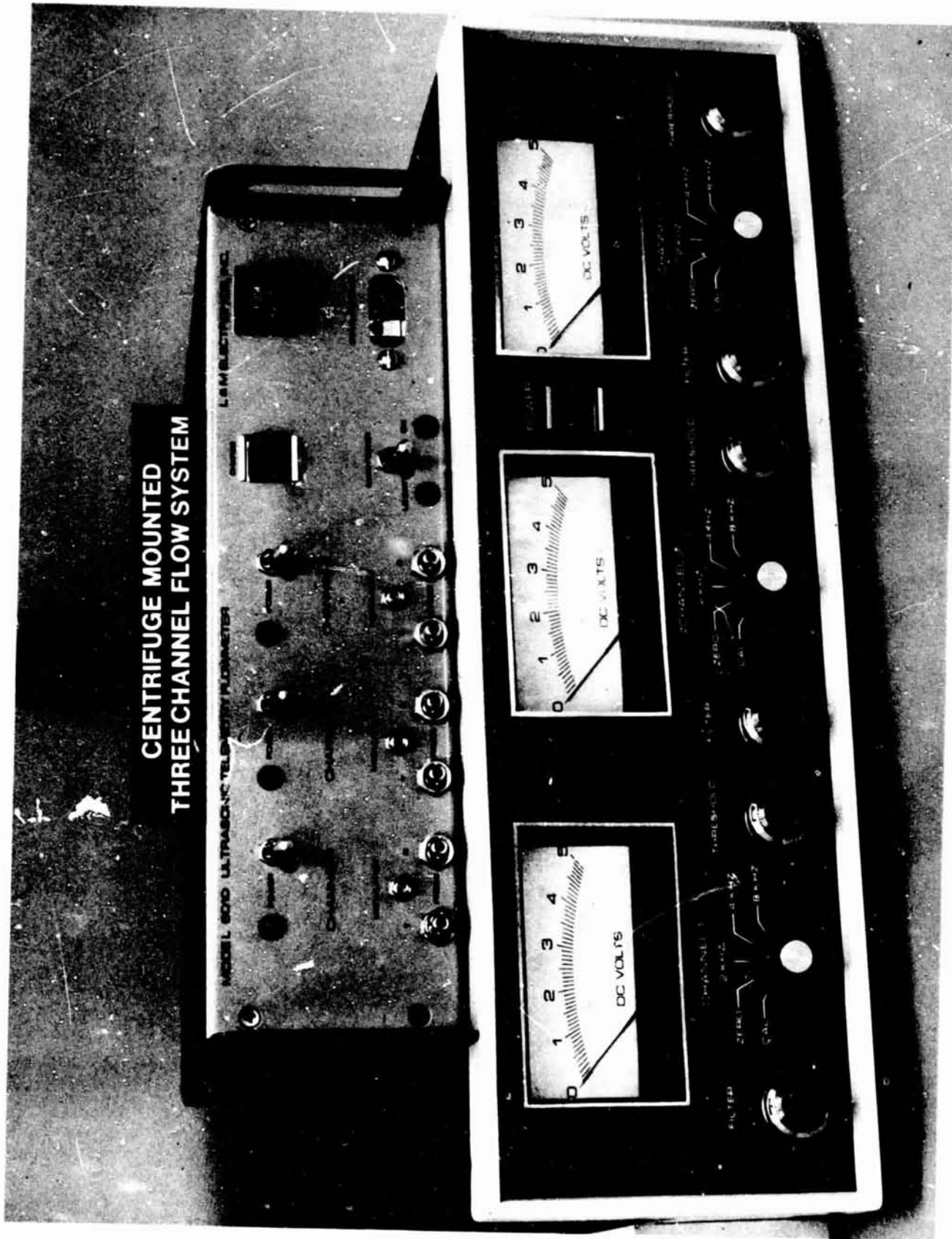


Figure 6. Ames three channel hardwire telemetry Doppler flowmeter.

separation of positive and negative Doppler shifts (Kalmus, 1955).

The sound scattered from a flow component can be expressed as:

$$E_j = A_j \cos 2\pi \left(F_C + \frac{F_C V_j}{C} \right) t$$

where F_C is the transmitted frequency; C is the velocity of sound in tissue; V_j is the velocity of scatter.

The Doppler shift $\frac{F_C V_j}{C}$ is obtained by separately multiplying E_j by $\cos 2\pi F_C t$ and $\cos (2\pi F_C t + \phi)$ since

$$\cos \alpha \cos \beta = 1/2 [\cos (\alpha + \beta) + \cos (\alpha - \beta)]$$

Thus,

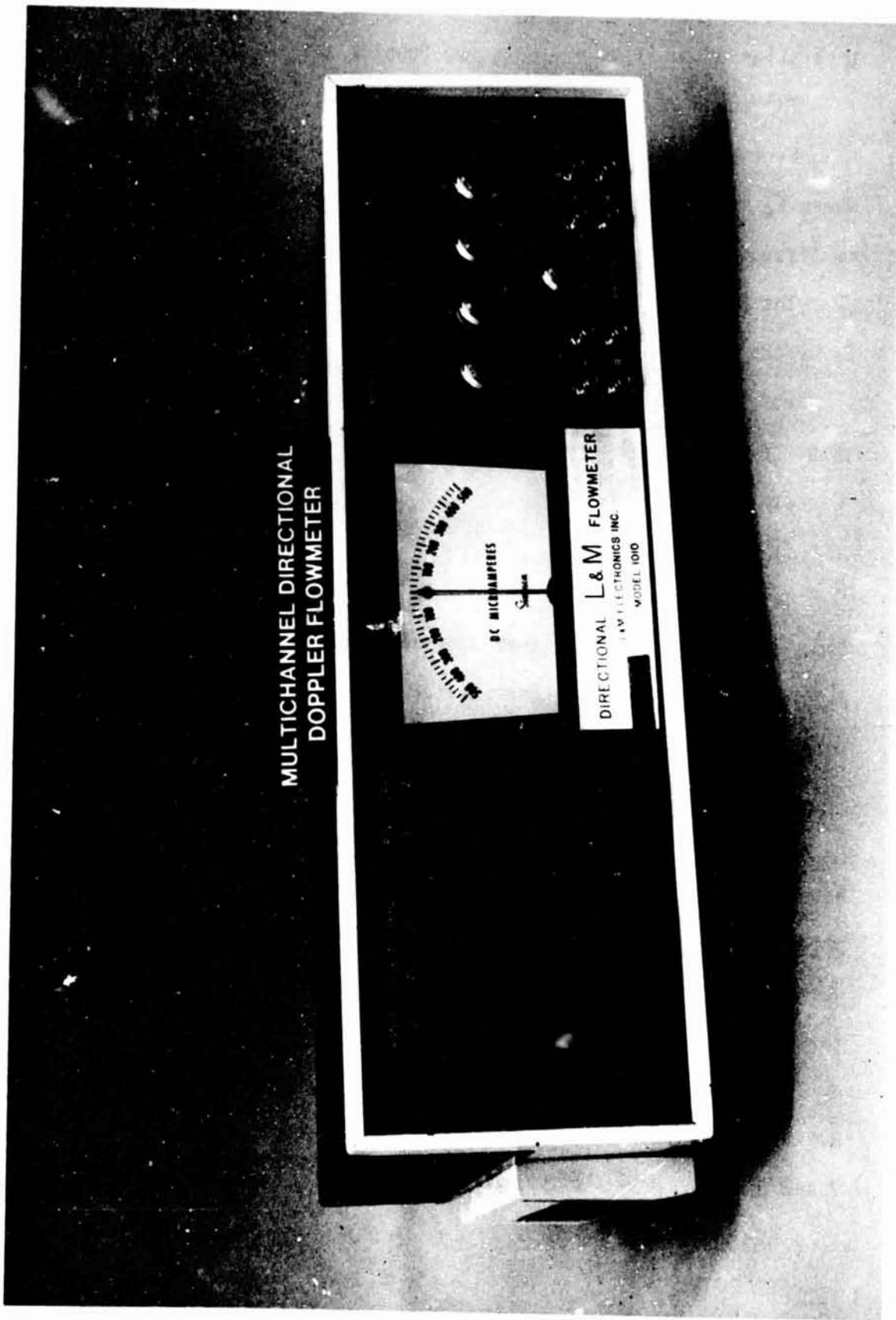
$$E_A = A_j \cos 2\pi \frac{F_C V_j}{C} t$$

$$E_B = A_j \cos 2\pi \frac{F_C V_j}{C} t + \phi$$

Depending on the sign of V , which indicates forward or reverse flow, the phase shift ϕ either adds to or subtracts from the Doppler shift. The non-phase-shifted signal E_A is used as a reference for determining the sign of ϕ .

The phase shift ϕ and thus the lead/lag phase relationship of E_A and E_B is easily determined by listening to the signals on stereo headphones. A logic circuit is used to combine E_A and E_B to produce voltages proportional to the mean forward and reverse velocity components. These voltages can be recorded separately as forward and reverse velocity or differentially as mean velocity.

Examples of direction-sensitive Doppler systems developed by NASA-Ames Research Center for centrifuge use are shown in Figures 7 and 8.



MULTICHANNEL DIRECTIONAL
DOPPLER FLOWMETER

DIRECTIONAL L & M FLOWMETER
L & M ELECTRONICS INC.
MODEL 1010

Figure 7. Ames four channel directional Doppler flowmeter for lab use.

MULTICHANNEL DIRECTIONAL DOPPLER FLOWMETER

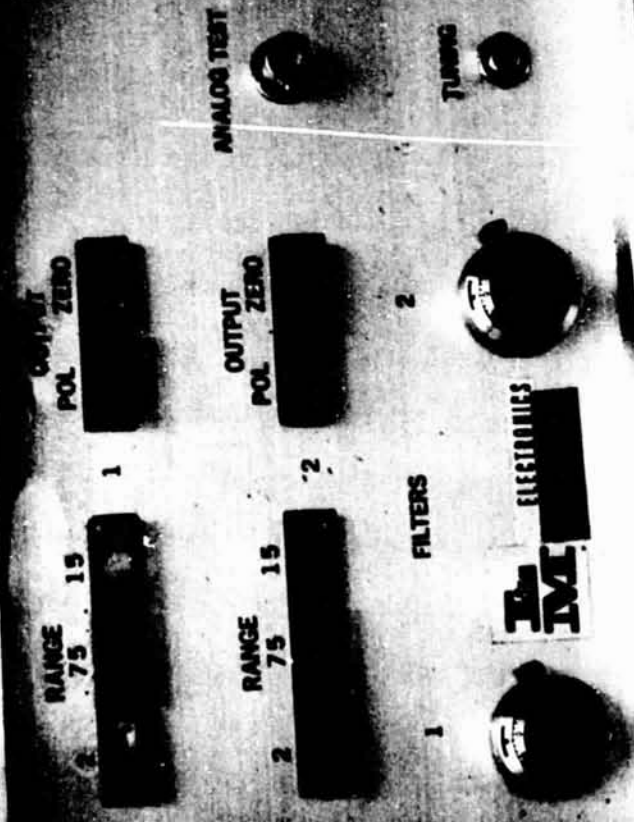


Figure 8. Ames two channel directional Doppler flowmeter for centrifuge use.

5.1.4 Doppler Audio

The analog blood flow velocity waveform forms an objective record of hemodynamic events; however, the audio Doppler shift signal in its unaltered state is very useful. Blood flow changes and reversals may be easily distinguished by listening to the characteristic changes in frequency. In clinical applications the Doppler flowmeter is almost always used in this manner as "blood flow stethoscope."

An important quality of the Doppler method then is the two-fold feature of graphic and audio records of hemodynamic activity. Both techniques are employed in this study.

5.1.5 Transducer Development

Several Doppler flow probes have been developed by the author and are reported by Mancini and Rositano (1973). Two variable angle devices, shown in Figure 9, were developed to determine the optimal piezoelectric crystal angles suitable for transcutaneous use over the temporal artery. Schlieren photographs were employed to determine and confirm crystal orientation and ultrasound depth of influence. Several dozen transducer design coupled with hundreds of applications on subjects at Ames Research Center resulted in the family of optimal transducer configurations shown in Figure 10. Beam width of 8 mm and 1-15 mm depth of focus was found satisfactory for 95% of the subjects.



Figure 9. Variable angle probes used to determine optimal crystal angles for final design.

TYPICAL TRANSCUTANEOUS PROBES

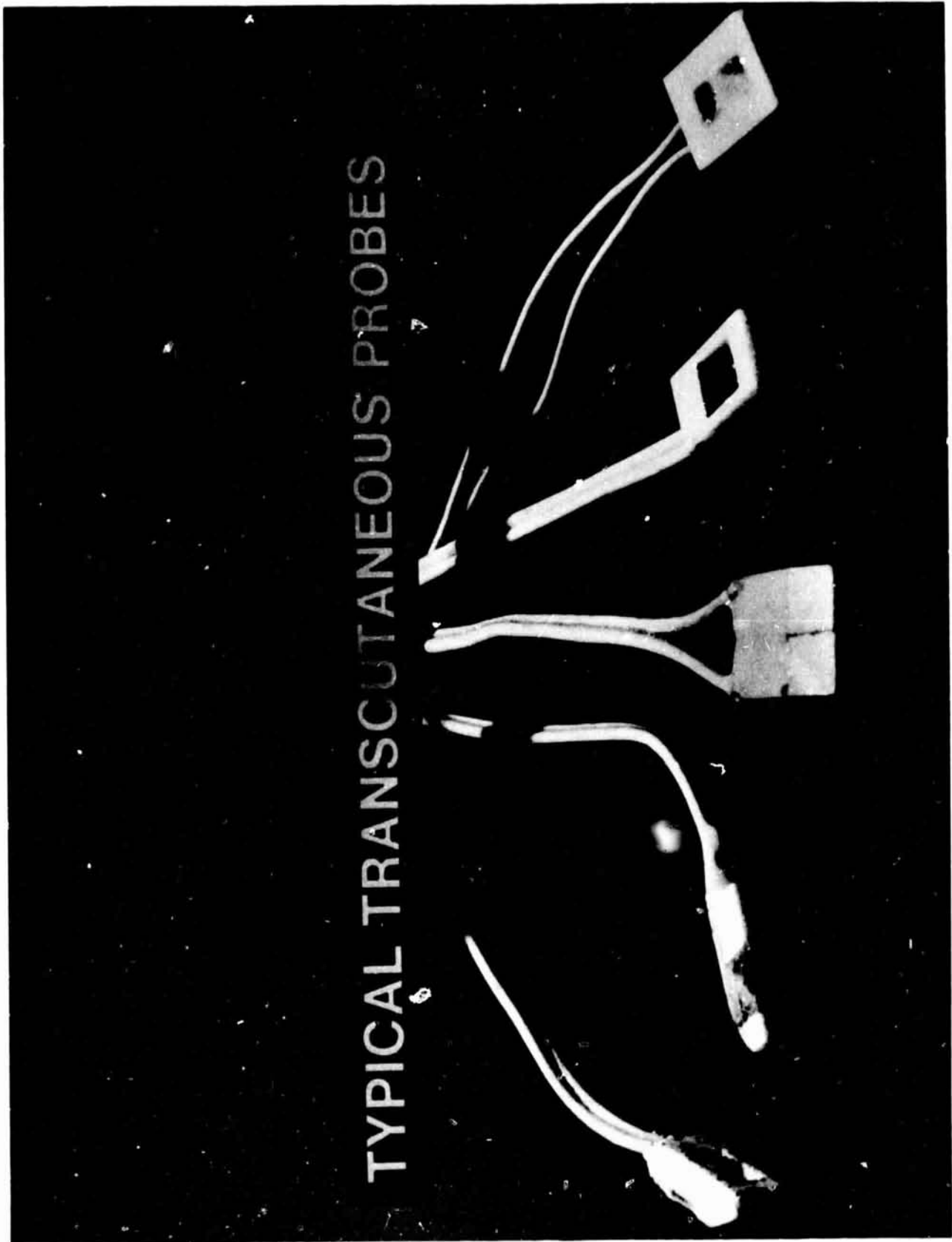


Figure 10. Typical ultrasonic Doppler blood flow probes for non-invasive use.

These transducers consisted of 8 MHz lead zirconate titanate (LTZ-5)* crystals mounted in a pre-cast styrofoam** housing. Ultra-flexible silicone rubber-jacketed shielded cable*** was used to minimize effects of acceleration on the sensor at high G.

5.1.6 Probe Attachment Over the Temporal Artery

For redundancy, both the left and right temporal arteries were instrumented. The areas above the right and left frontal branches of the superficial temporal arteries were palpated. The skin above the maximum pulse was then shaved, if necessary, to ensure good acoustic coupling. The transducer cavity was filled with a water-soluble transmission gel,**** and the transducer was secured to a transparent double-backed adhesive disc and then moved about the area until the strongest audible Doppler signal was detected. The location was marked with an indelible pen and cleaned with isopropyl alcohol (Figure 11). The water soluble gel was removed from the transducer cavity and replaced by a high-viscosity acoustic gel.***** Care was taken to exclude all visible air bubbles. The backing on the adhesive disc was removed and the transducer secured to the premarked area using transparent surgical tape for reinforcement (Figures 12 and 13).

*Transducer Products, Torrington, Conn.

**Dow Corning, Midland, Mich.

***Calmont Wire and Cable, Santa Ana, CA

****Aquasonic 100, Parker Lab, Irving, NJ

*****Gelsonde, Hoffman LaRoche, Nutley, NJ



ORIGINAL PAGE IS
OF POOR QUALITY

5.2 Centrifuge Facilities

Two centrifuges were used for this project. Several hundred low G, gradual onset (≤ 0.1 g/second), Space Shuttle reentry-type runs were conducted on the 20 G, 15.2 meter diameter centrifuge at NASA-Ames Research Center, Moffett Field, California. Although feasibility of using the Doppler flowmeter on the temporal artery at G was proven at Ames by Rositano and Mancini (1972), validation and comparison with previous methods were obtained from subjects riding on the USAF School of Aerospace Medicine (USAFSAM) human centrifuge with a radius arm of 6.1 meters. See Figures 14 and 15.

At Ames the subjects were positioned on a specially-made, stationary couch, fixed at an appropriate angle, so as to provide the desired head to foot ($+G_z$) resultant vector (see Figure 16). Subjects at USAFSAM were seated upright, in a seat with a 13° back angle (see Figure 17). The gondola is free-swinging and counter weighted at its base to produce a resultant vector in the $+G_z$ direction. The $+G_z$ level was determined by an accelerometer placed at the subject's mid-chest level.

5.3 Subject Safety

All subjects were instrumented with two channels of EKG (sternal and biaxillary) using conventional silver-silver chloride electrodes. Heart rates and cardiac rhythm were obtained from the EKG records. Voice, visual, and closed circuit television contacts



Figure 14. N A S A-AMES 20 G Centrifuge.

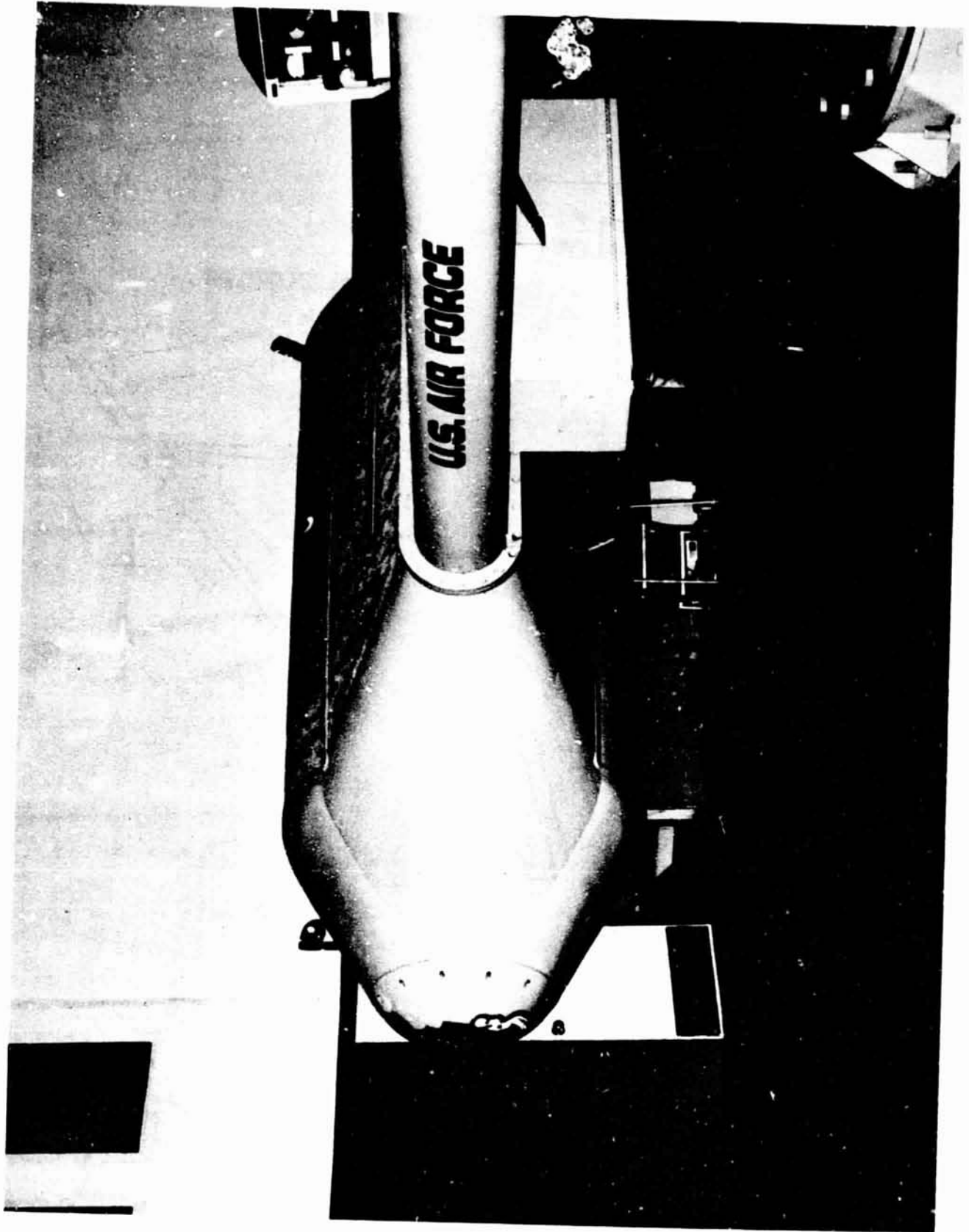


Figure 15. Human centrifuge at USAF School of Aerospace Medicine, Brooks AFB, Tx.

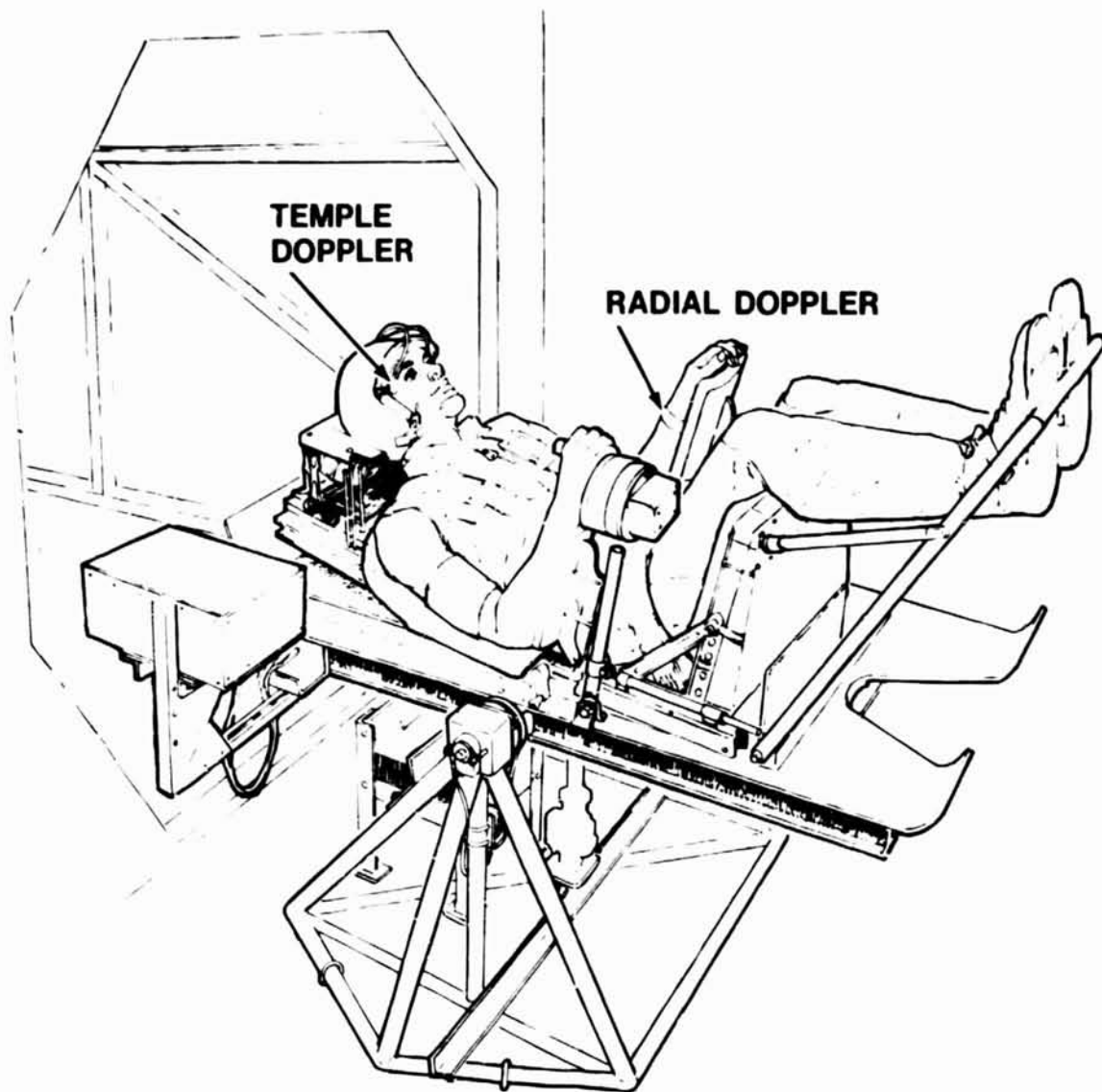


Figure 16. Subject seating on 20G centrifuge at NASA AMES.
Chair is fixed at appropriate angle to cause head to foot G vector.

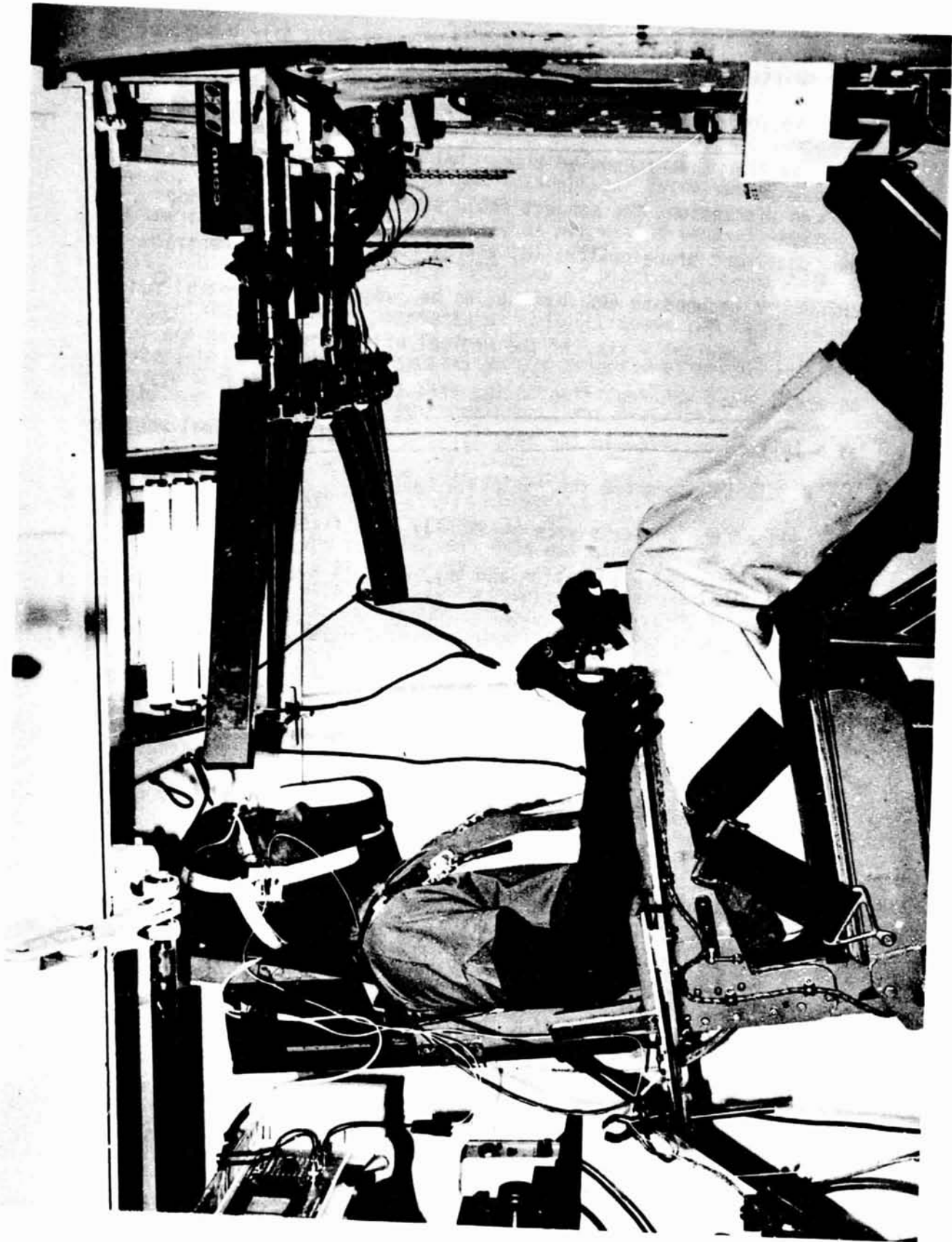


FIGURE 17. Subject seating in gondola of USAF SAM human centrifuge.

were maintained with subjects at all times.

The following criteria were established for stopping a run at an earlier-than-scheduled time: (a) subject's choice - viz, at his own discretion, the subject could stop the run by releasing the "dead man" brake switch; (b) vision - viz, subject's central vision was reduced to 50% dimming, as he judged by the central red light; (c) medical - viz, if the medical officer monitoring the run observed gross abnormalities in the EKG; and (d) technical - viz, if a failure occurred in the data system, so that the medical monitor was unable to guarantee the subject's safety.

All of the subjects were physically qualified by a Class I or Class III physical examination and they were 18 to 36 years old.

5.4 Conventional Visual End Point Apparatus

The cockpit instrument panel was equipped with standard black-out lights; two green lights for peripheral vision and one central red light for fixation. The three lights were mounted on a 76 cm horizontal, off-white bar which was positioned approximately 69 cm from the subject's eyes. This bar was adjustable so that it was on a horizontal plane with the eyes, and the visual angle subtended at the bridge of the subject's nose by the green lights was 54°. The interior of the gondola is painted an off-white color and

illuminated with nine ceiling fluorescent lamps (14 W). At the subject's eye level, illumination was 40 foot candles.

Disappearance of the green lights as perceived by the subject was classified as peripheral light loss (PLL). Perceived dimming of the central red light to a 50% level was called central light loss. To avoid confusion in terminology of blackout a percentage of light loss was found appropriate: 50% CLL means red light appears to have reduced intensity to 50% of original brightness while 100% CLL means no light remaining (true blackout!).

5.5 Data Acquisition

At both Ames and USAFSAM, all data was simultaneously recorded on a Brush MK200, eight-channel recorder and a Sangamo 4700, 14-channel analog magnetic tape recorder. A list of information recorded for each study will be covered in Chapter 6.

6.0 EXPERIMENTAL METHODS

Six experiments were required to adequately assess the feasibility, scope of use and applications of the proposed technique. Experimental methods and observed results are presented as a unit for each study. An integrated discussion of all results is presented in Section 7.0.

A restatement of overall study objectives may be helpful before presenting the record of experiments:

To examine the efficacy of a transcutaneous Doppler flowmeter to monitor superficial temporal artery blood flow velocity during acceleration, to correlate results with existing objective and subjective techniques, and to evaluate the method for anti-g countermeasure procedure evaluation.

6.1 Preliminary Test at Ames Research Center

Basis for the several experiments to be described came from two years of preliminary work at Ames Research Center in a comprehensive program headed by Harold Sandler, MD, to assess cardiovascular stress effects of weightlessness. One phase of the Ames project was characterization of peripheral vascular hemodynamics during weightlessness and simulated reentry.

During several hundred centrifuge runs with 24 subjects at Ames, Doppler transducers were evaluated on numerous body

sites. Criterion for final site selection, in addition to cardiovascular significance, included sensor attachability, long-term comfort, and reliability for continuous and repeatable measurements. A special helmet was also fabricated with barn-door flaps to accommodate sensors near the ear. External carotid artery blood flow was most difficult to continuously monitor.

Subjects used in the Ames tests had no previous centrifuge experience. Training runs to blackout, 100% central light loss (CLL), were made to establish a control tolerance level (time to blackout) and to acquaint the subjects to the physical sensations of centrifugation.

6.1.1 Results of Ames Tests

The brachial, radial and frontal branch of the superficial temporal arteries were the most consistently accessible sites suitable for instrumentation. It was observed that (a) brachial and radial arterial flow measurements reflected significant cardiovascular changes occurring during and after acceleration. Flow decreased in both of these vessels under the influence of acceleration and showed a definite compensatory increase in flow when the stress was removed (Figure 18(b)). However, these signals proved to be poor indices of the onset of greyout (peripheral light loss) or blackout. In most cases, flow continued although at a diminished level during blackout, and in one case, even during unconsciousness. However, temporal artery blood flow

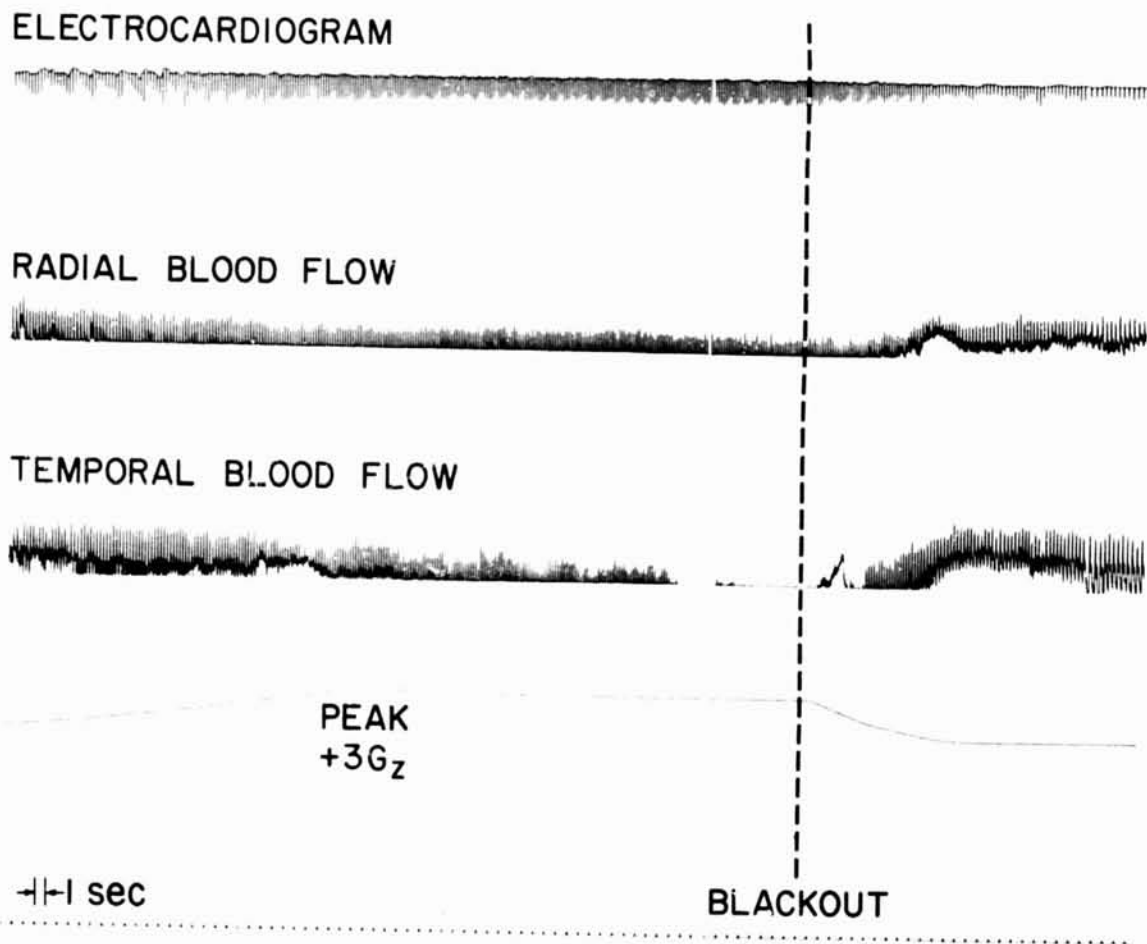


FIGURE 18. Comparison of radial and temporal arterial blood flow velocity during gradual onset run.

showed a consistent correlation between subjective peripheral light loss and cessation of flow in the artery. Cessation preceded blackout by 2 to 20 seconds (Figure 18(c)). The audible Doppler sounds were heard to have a characteristic sound late in diastole as an end point was reached. *A hypothesis was that the sound and flow changes late in diastole might evidence flow reversal reported by Leverett (1971) in his classic photographic study of retinal blood flow at blackout.*

Data from approximately twenty percent of the test subjects was inconclusive. A typical run of this type would end with the subject reporting an end point while temporal flow was still present. Lack of centrifuge experience, on the part of these subjects, as well as the newness of the Doppler/temporal artery flow technique, made resolution of the discrepancy impossible. Verbal questioning after a run of these subjects did reveal some hesitancy to discretely describe a clear end point phenomena.

The Ames results, although sufficient to indicate feasibility, clearly identified the need to validate the method on experienced centrifuge subjects at various G levels and profiles. Dr. Sidney Leverett offered to provide the facilities and experienced centrifuge test subject panel at the USAF School of Aerospace Medicine, Brooks AFB, Texas. The data and results to follow were obtained in joint NASA/USAF tests conducted on the USAFSAM human centrifuge.

6.2 Methods for Correlating Temporal Flow Velocity and Direct Eye Level Blood Pressure

Seven healthy male volunteer subjects, ages 21 to 25, were studied. All had passed a USAF Class II flying physical examination and had extensive centrifuge experience. Subjects were instrumented as previously described (Sections 5.1.6 and 5.3).

A directional signal processor was used with one temporal transducer, while a non-directional processor was used with the other (Models 1012 and 6010, respectively, L&M Electronics, Daly City, CA). The directional Doppler instrument previously used at Ames for chronic flow studies on animals (Rositano, 1973) was improved for transcutaneous use in the NASA/USAF tests to evaluate the reverse flow hypothesis suggested in the Ames tests.

The right radial artery was catheterized, using a Longdwell Teflon 20 gauge cannula. Eye level arterial blood pressure was measured with a miniature strain gauge transducer (Model P37, Statham Instruments, Oxnard, CA), mounted at eye level and connected to the radial artery catheter by a short polyethylene connector. The diaphragm of the transducer was oriented parallel to the G vector. A three-way stopcock was used at the cannula for flushing the catheter with heparinized saline. The velcro head harness and eye level pressure cell holder are shown in Figure 19.

Rapid and gradual (ROR and GOR) onset runs were used to stress subjects to the point of visual failure. The light bar configuration used by the subjects to determine peripheral light loss (PLL)



Figure 19. Velcro harness for eye level arterial pressure cell.

and central light loss (CLL) has been previously described (Section 5.4). ROR's were begun with 2.5 G for 15 seconds and increased in increments of 0.5 G until peripheral light loss occurred; at this time, runs were increased by 0.2 G until the end point of blackout (50% loss of central light). Subjects then underwent a GOR to blackout. Adequate time was allowed between runs for the subject to return to a normal physiologic state.

6.2.1 Results - Diastolic Reverse Flow Hypothesis

The previously heard and observed changes in flow late in diastole at increased G were clearly identified to be retrograde blood flow as shown in Figure 20, thus confirming the earlier hypothesis. In the audio record of the Doppler shift, the higher frequency sounds of blood flow during systole are gradually replaced by the lower frequency sounds of reverse flow. Diastolic retrograde eye level blood flow was observed to increase with G level.

6.2.2 Results - Rapid Onset Runs (ROR)

When blackout was approached (range 2.7 to 4.6 G), eye level arterial blood pressure (Pa) began to fall concomitant with the occurrence of retrograde flow in the temporal artery (Figure 21). Zero forward temporal artery flow (\dot{Q}_{ta}) was determined by both graphic and audio recordings six seconds (range 4-9 sec.) prior to

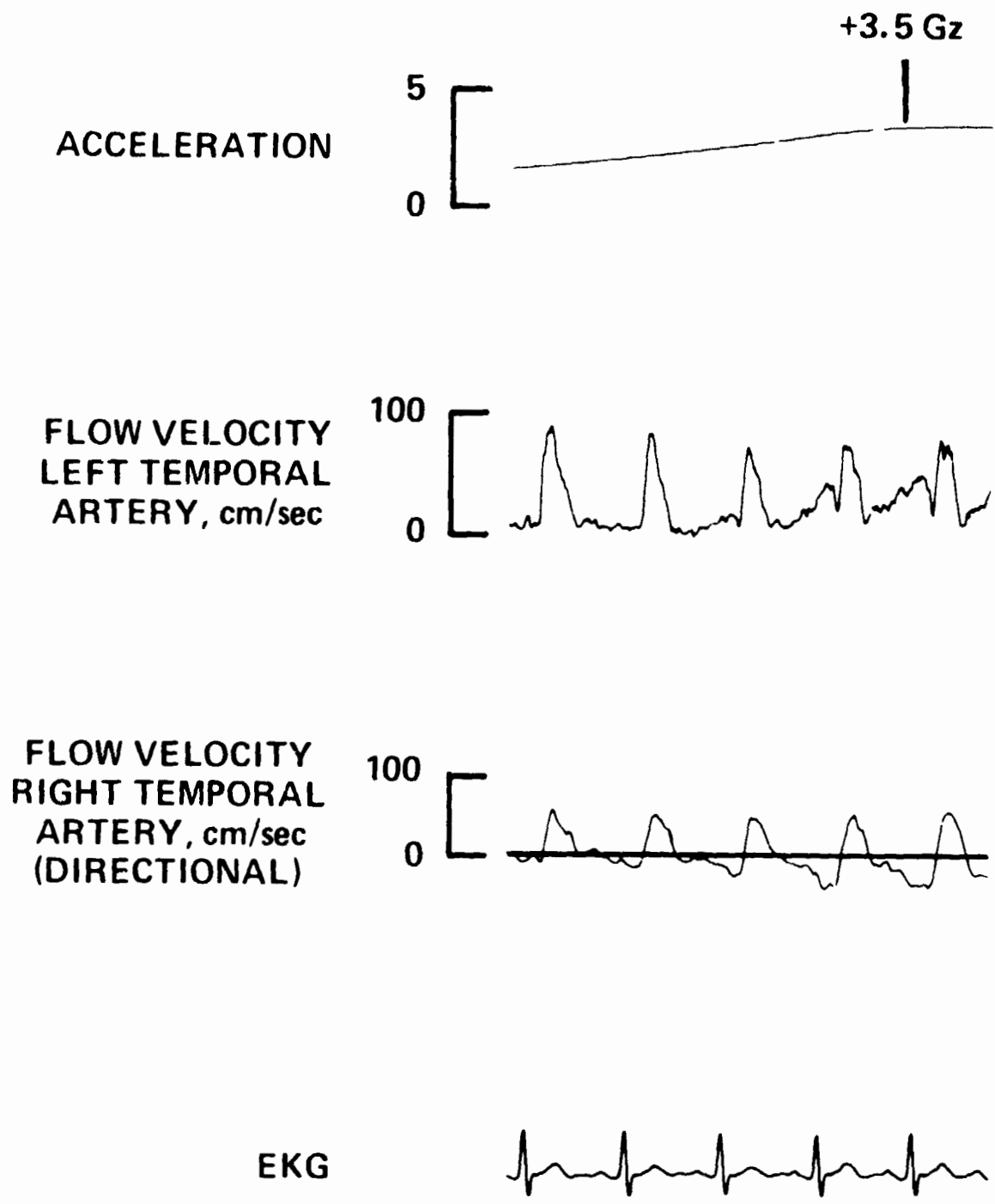


Figure 20. Retrograde eyelid blood flow velocity is confirmed.

blackout. Eye level mean arterial pressure (Pa) decreased to 20 ± 1 mmHg (n=16) when zero forward \dot{Q}_{ta} was initially recorded. Arterial pressure and temporal artery flow velocity increased simultaneously during centrifuge deceleration, with a significant increase in pressure and flow velocity occurring post run when compared to previous values.

An interesting correlation of pressure and flow with latency in subjective visual symptoms is shown in Figure 22. Rapid onset run A (ROR A) was terminated by the subject at 100% central light loss five seconds after zero \dot{Q}_{ta} ; whereas, ROR B was terminated one second after zero \dot{Q}_{ta} by the medical monitor with no visual symptoms.

6.2.3 Results - Gradual Onset Runs (GOR)

The correlation of Pa, \dot{Q}_{ta} and visual symptoms recorded during ROR's was not duplicated to the same degree during GOR's. Three of the seven subjects had clearly identifiable Doppler end points. From one of these three subjects, a net negative mean flow rather than complete cessation was recorded seven seconds before blackout; that is, retrograde diastolic flow exceeded forward systolic flow (Figure 23). Results for the other four subjects were varied: Subject 1 - Pa and \dot{Q}_{ta} varied with respiratory cycles; Pa varied between 20-25 mmHg for 11 seconds pre-blackout; the retrograde flow component of the \dot{Q}_{ta} wave was building during this period. Subject 5 - zero forward \dot{Q}_{ta} was never achieved;

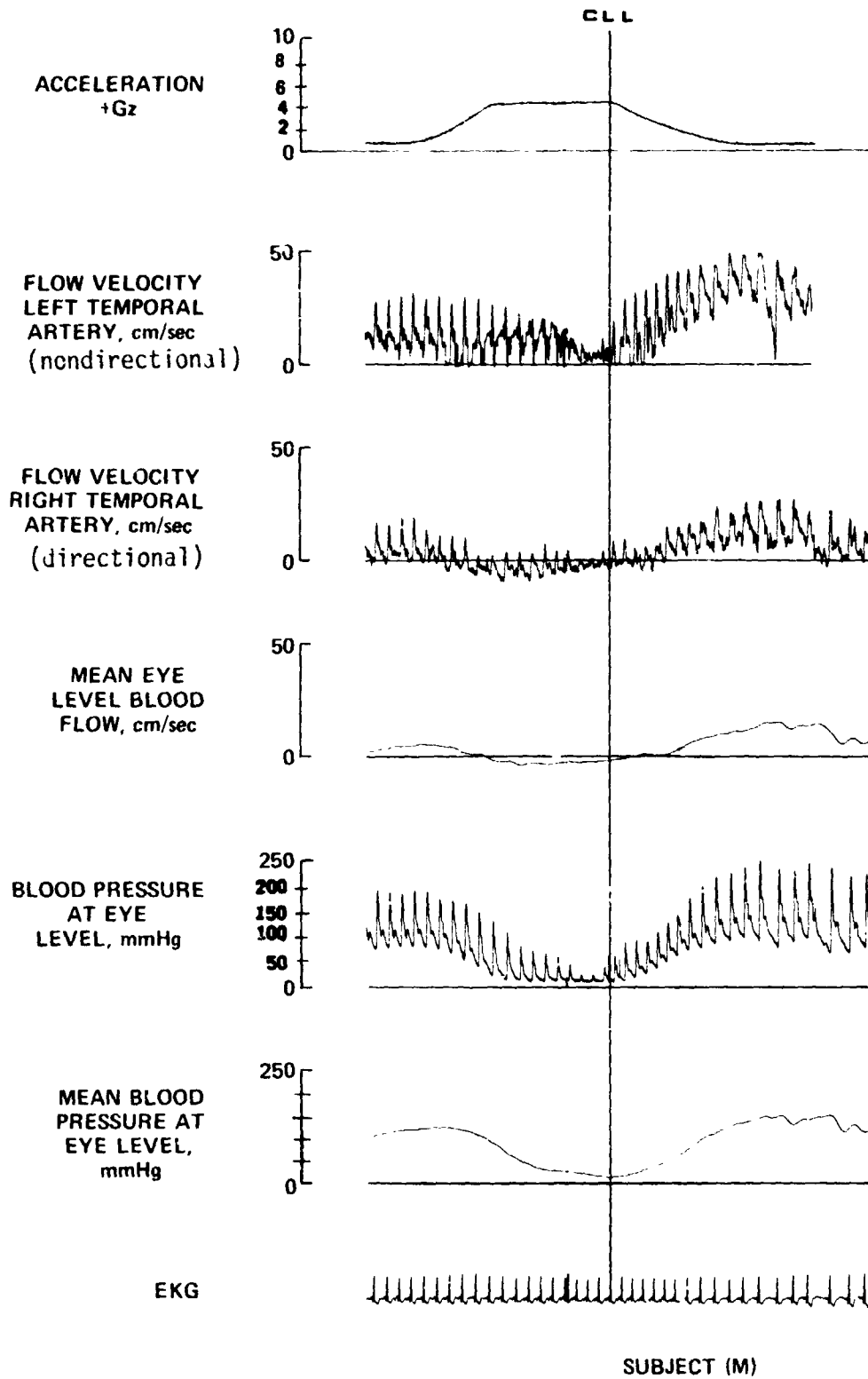


Figure 21. Effect of rapid onset acceleration on eye level blood pressure and flow velocity.

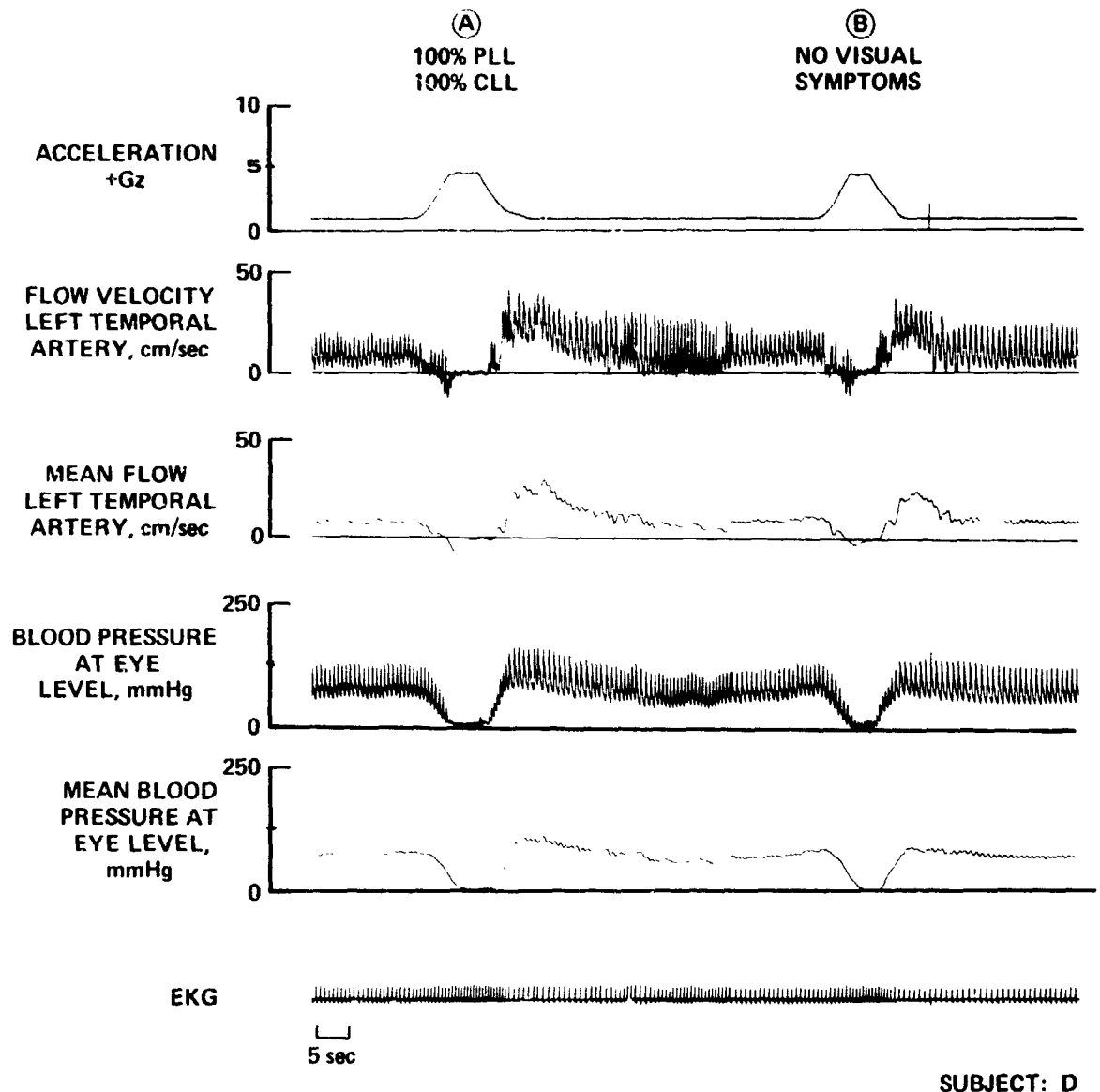
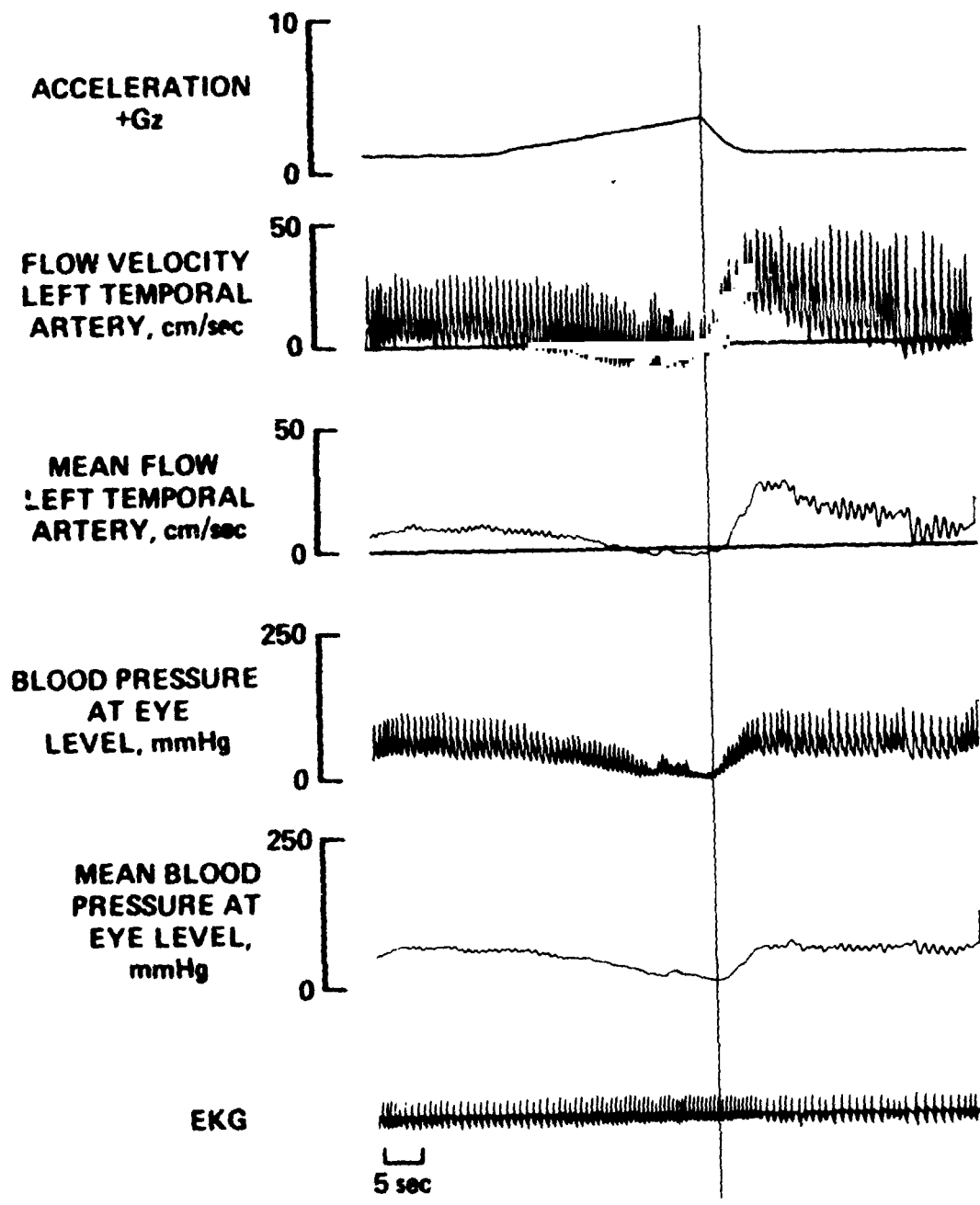


Figure 22. Latency of visual response. Subject reported 100% loss of lights at end of run A; however, no visual symptoms during run B ended by medical monitor.



SUBJECT: J. C. W.

Figure 23. Negative mean blood flow velocity 7 seconds prior to blackout during gradual onset run.

Pa was never below 30 mmHg. Subject 6 - Pa was at 20 mmHg or below for nine seconds pre-blackout; zero forward \dot{Q}_{ta} was never attained; however, the retrograde flow portion of the \dot{Q}_{ta} wave had become dominant. Subject 7 - \dot{Q}_{ta} flow pattern was very much like subject 6; zero forward \dot{Q}_{ta} was never attained, but a progressively increasing back flow was seen prior to blackout (Pa = 30 mmHg at blackout). Pa had been increasing and decreasing with respiratory cycles prior to this time.

Because of the subjective nature of CLL determination by the subject, there was no conclusive way to evaluate difference between the reported end point and Doppler data. Another experiment (6.3) would have to be conducted to resolve the problem.

6.3 Critical Evaluation of GOR End Point and Temporal Blood Flow

This test was designed to evaluate the conditions present at CLL for the gradual onset profiles using first the test subject's criterion for CLL (as in 6.2), and in a subsequent run, loss of temporal blood flow as an objective end point.

Eight experienced centrifuge subjects were instrumented as previously described. During the first of two GOR's (0.1 g/sec) each subject was asked to terminate his run when he perceived a 50% CLL; whereas, the second run was to be terminated by the medical monitor using objective analysis of temporal flow data.

For safety, at no time was the central light to degrade beyond 60% as defined by the subject. The Doppler system was non-direction-sensitive; however, retrograde flow during diastole was easily distinguished from forward flow as previously described (Figure 20).

6.3.1 Results

Subjective CLL end points for five of the eight subjects in the first GOR coincided with objective predictions of temporal blood flow; however, three subjects terminated their runs at a time when temporal flow had not reached sustained retrograde or zero flow. In the subsequent run terminated by the medical monitor by objective analysis of flow data, all eight subjects reported visual loss between 45% and 60% CLL. Typical data from both runs of one of the three uncertain subjects is compared on Figure 24. Flow velocity at subjective blackout in Run 1 does show reversal during diastole and a decreasing overall amplitude; however, no clear end point is identifiable. In the second run, the flow data clearly indicates an end point.

6.4 Correlation of Temporal Artery and Common Carotid Artery Flow During +G_z

Development of a transducer by R. M. Olson, et al (1973) for transcutaneous carotid flow velocity measurement made possible the comparison of the temporal and carotid arterial flow patterns at G.

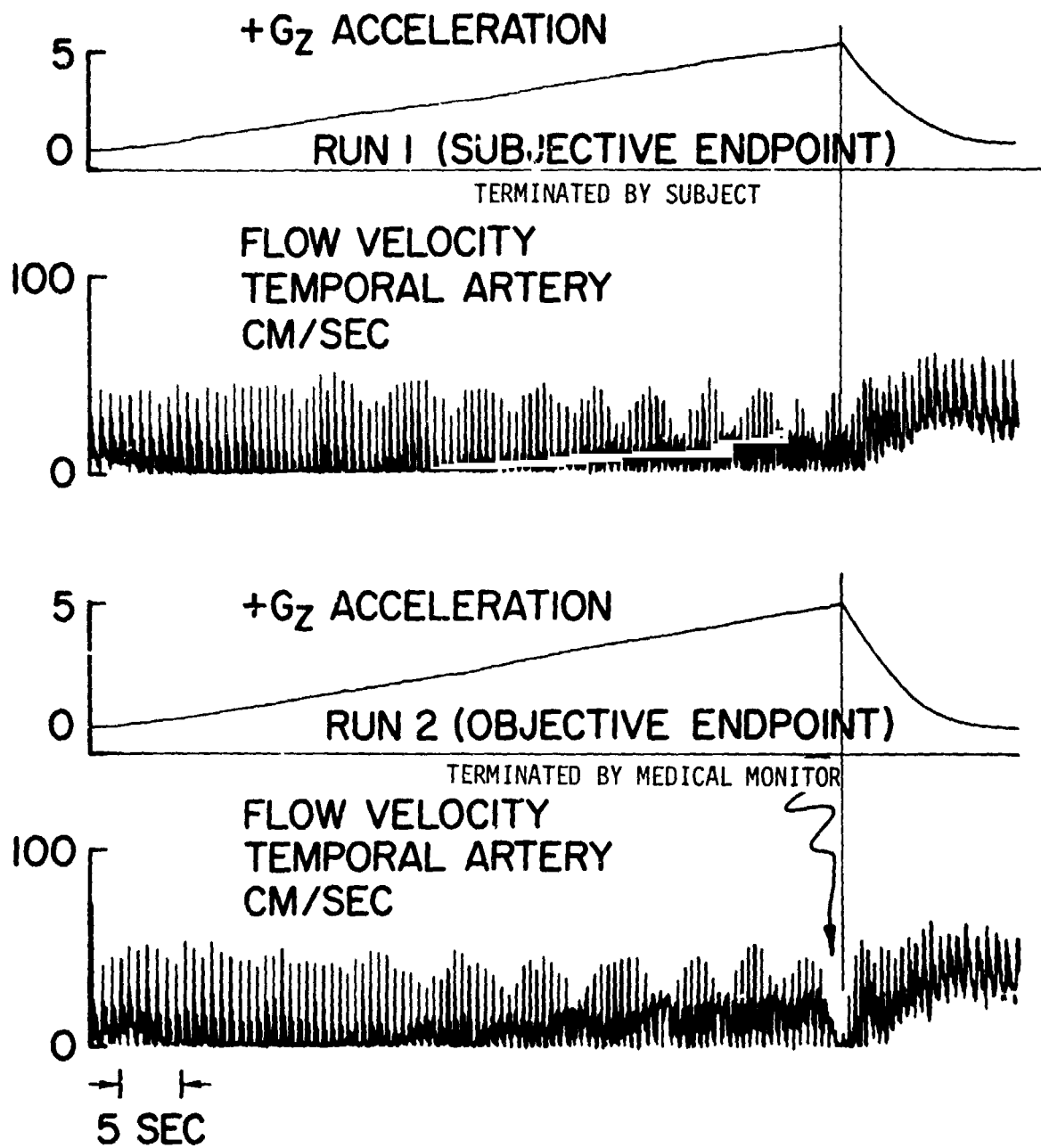


Figure 24. Comparison of subjective and objective endpoints during gradual onset runs.

The carotid sensor consists of an ingenious steerable module, containing two piezoelectric crystals, mounted on a two-inch-wide velcro neck strap.

The eight subjects used in the previous study were reinstrumented with Doppler flowmeters over the common carotid as well as the temporal artery. Only one directional channel was available; therefore, it was used on the carotid sensor to confirm flow direction. Rapid onset runs (1 G/sec) and gradual onset runs (0.1 G/sec) were used to produce stress to visual failure.

6.4.1 Results

Some difficulty was experienced keeping the carotid sensor in place at G. The mass of the metal swivel portion of the probe was apparently sufficient to cause movement relative to the skin at G. Slight compression of the subject's neck area at G was observed via the television monitor. Swallowing also affected the transducer-artery alignment, producing a periodic artifact in some data. Artifact-free data was obtained from four subjects.

Carotid artery flow velocity exhibited retrograde activity corresponding to diastolic retrograde flow in the temporal artery as shown in Figure 25. Retrograde carotid flow was only observed during the peak retrograde activity in the temporal artery. As temporal flow progressed toward cessation, carotid flow returned to 100% forward direction.

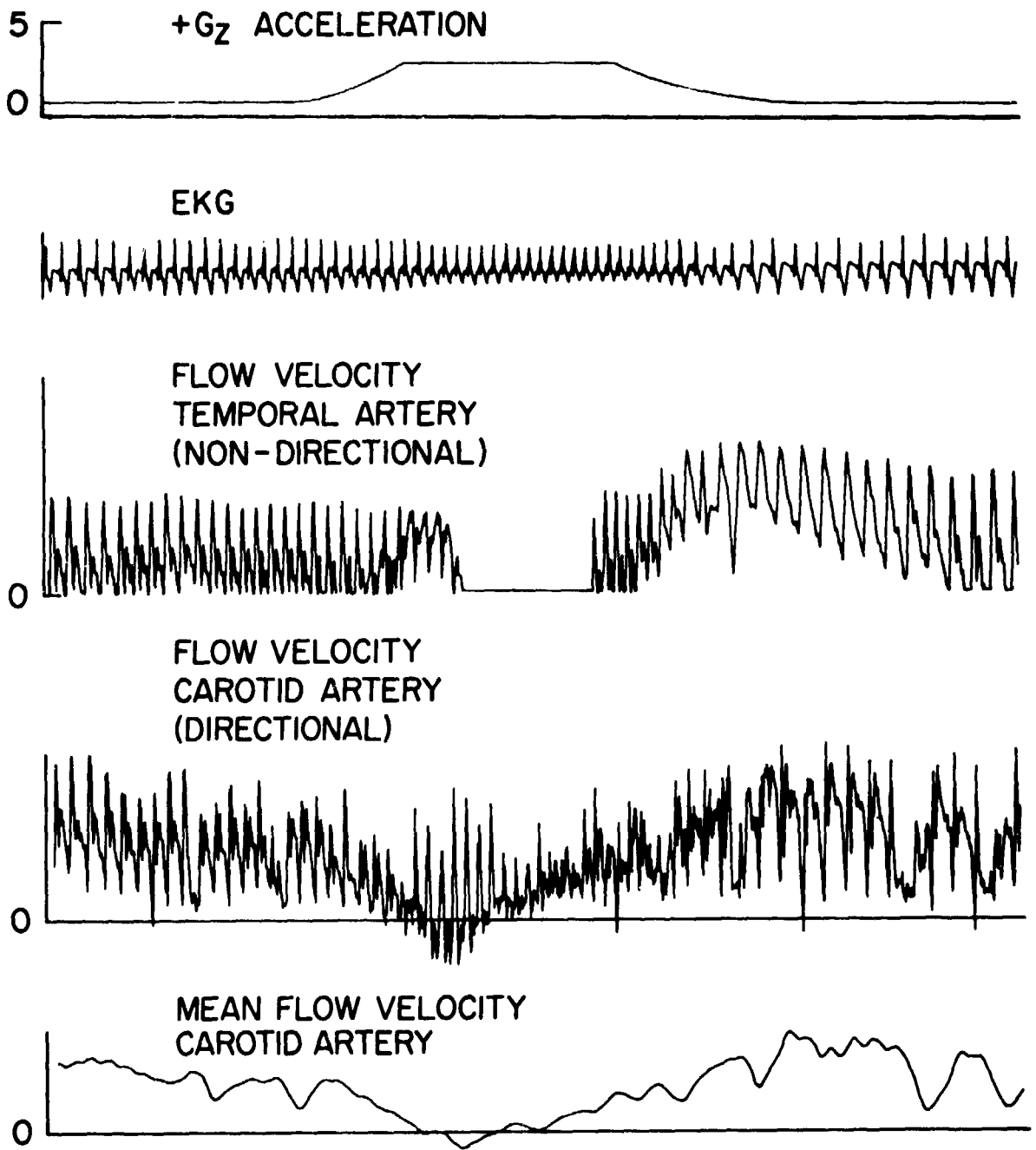


Figure 25. Comparison of carotid and temporal arterial blood flow velocity during rapid onset run.

6.5 Correlation of Temporal Artery Flow and Objective Visual Field Limit

Previous studies using a transcutaneous ultrasonic Doppler blood flowmeter over the temporal artery have confirmed a relationship between loss of central vision and discrete changes in eye level blood flow velocity. As central light loss (CLL) is approached temporal artery flow velocity first reverses direction during diastole and progressively decreases toward total cessation several seconds before CLL.

If the temporal artery Doppler technique is to provide an indication of visual field change prior to CLL, an accurate appraisal of the progressive loss of peripheral vision and its relationship to temporal blood flow must be made. The conventional light bar, using a central red light and two peripheral green lights, does not permit high resolution tracking of peripheral light loss. This study was to analyze the relationship between temporal flow velocity, eye level arterial blood pressure, and progressive degradation of the visual field.

The Gillingham light bar shown in Figure 26 provided a means for high resolution tracking of visual limits in the horizontal plane. The two peripheral green lights were replaced with a linear array of sixty white lamps on a two-inch-wide semicircular bar extending to 60 degrees each side of a central red fixation light. The lamps are automatically sequenced beginning with the

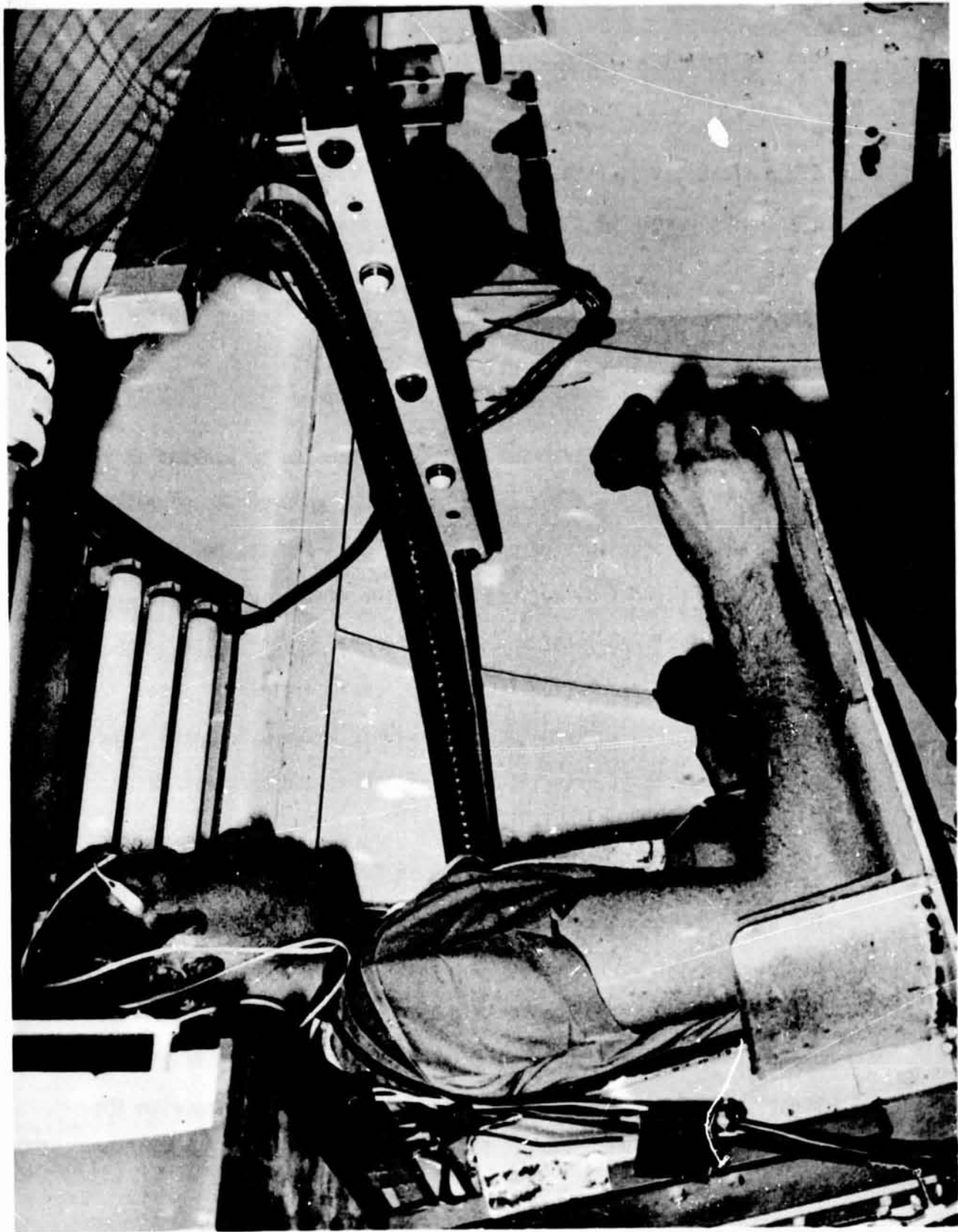


Figure 26. Gillingham 1200 Light bar mounted above standard light bar- IISAF SAM

outermost lamps progressing toward the center red light. The subject activates a switch when light enters his visual field, causing the lights to reverse course and retrace toward the lateral limits of vision. When the light recedes beyond the visual field the switch is again activated and the process is repeated. Objective positional information of the horizontal visual limits is continuously recorded as the lights sequence back and forth about the point of vision loss.

Eight subjects were instrumented as previously described in Section 5. Right radial artery was catheterized in the same manner as described in Section 6.2. All subjects were experienced in use of the new light bar. Three acceleration profiles were used, consisting of ROR's, GOR's and variable G similar to high performance aircraft maneuvering (GOG). As an adjunct to the test, cardiovascular and visual response to 45° and 65° seat back angles (in addition to standard 13°) were evaluated. Response to seat angle change will be presented in Section 6.6.3.

6.5.1 ROR Results

A typical ROR to blackout is shown in Figure 27. Retrograde flow begins when diastolic pressure decreases below 35 mmHg at eye level. Zero forward flow is seen as systolic pressure drops to

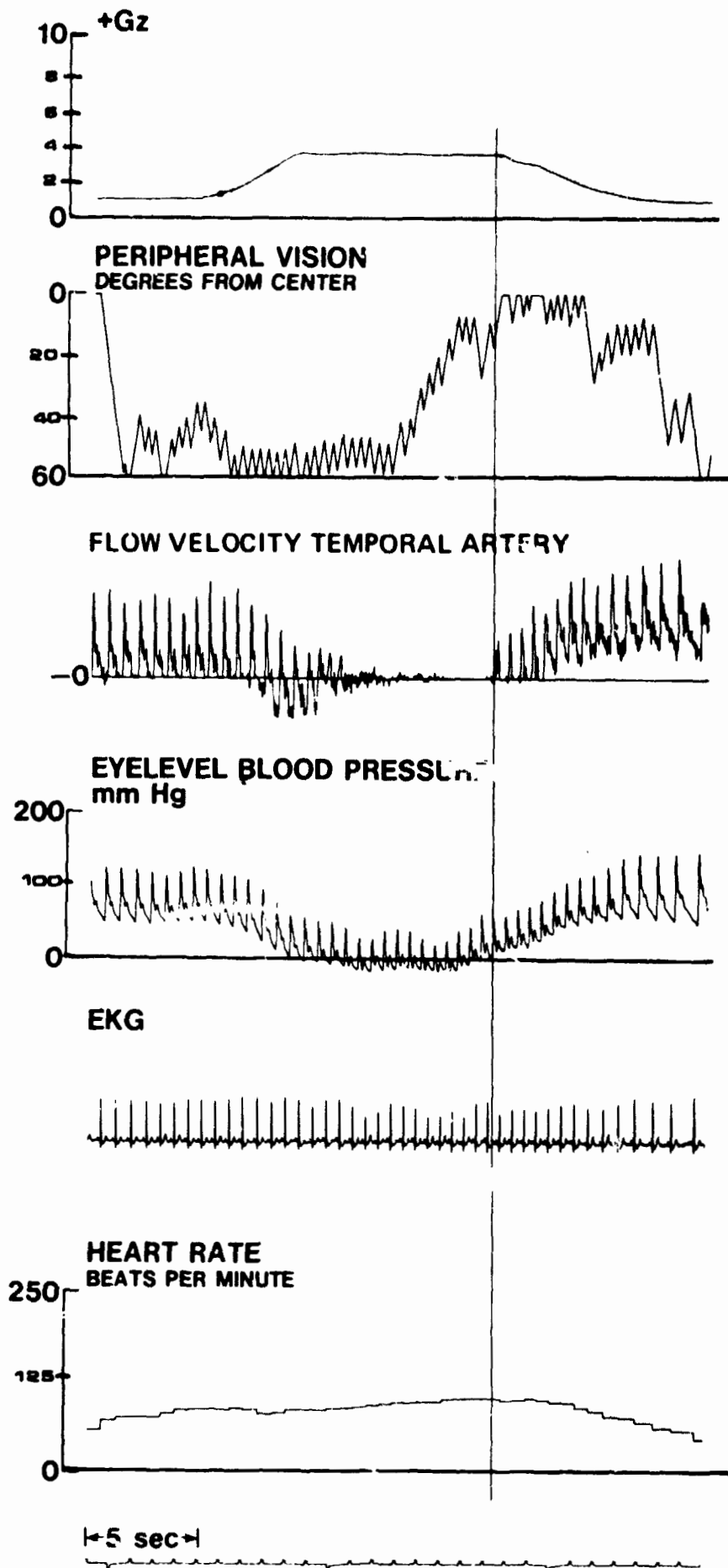


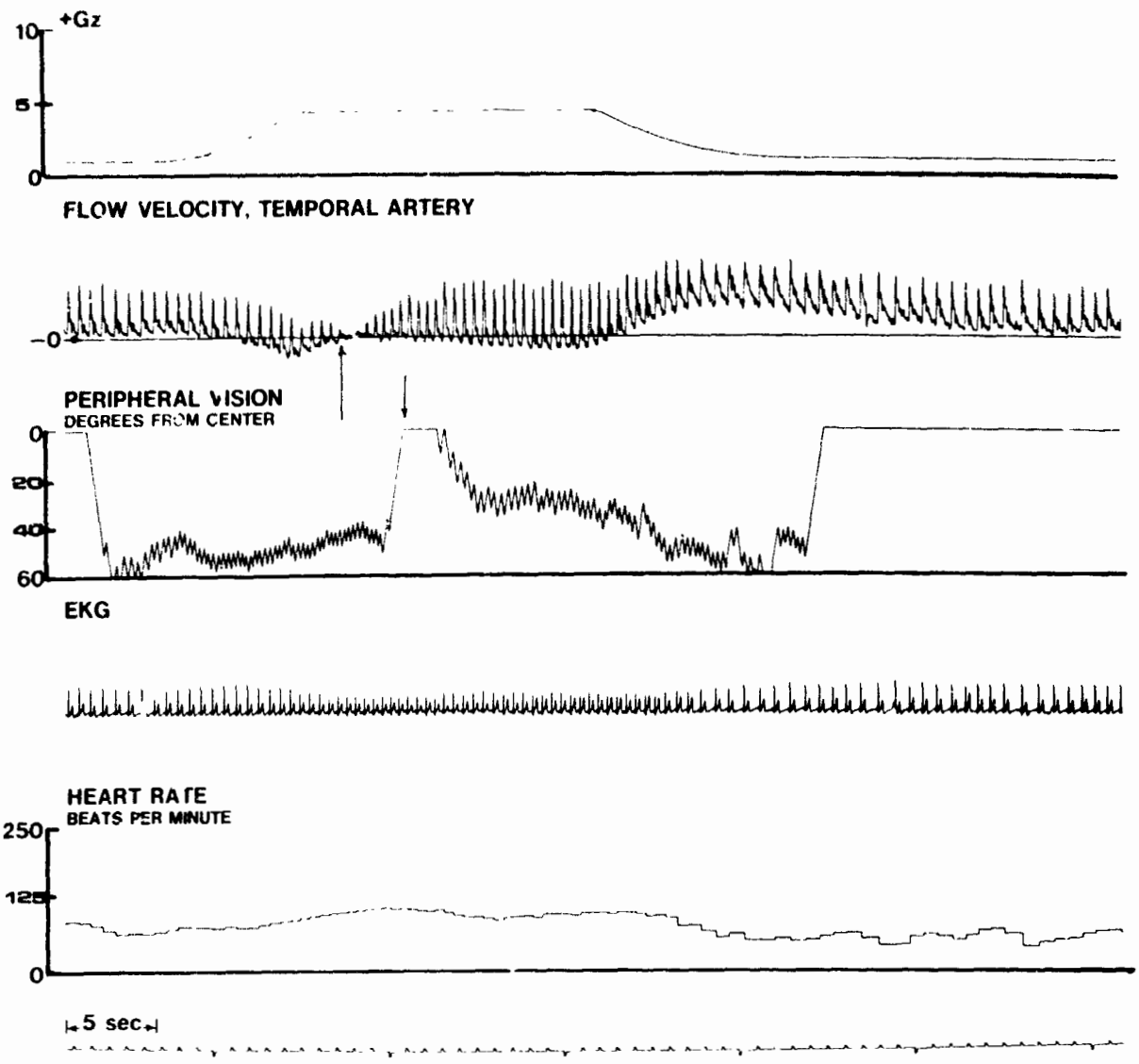
Figure 27 Correlation of visual response with blood pressure and flow velocity during rapid onset run.

22 mmHg. Negative mean blood flow velocity is observed 5.6 seconds (range 4 to 8) seconds prior to visual field change perceived by subject.

For ROR's to G levels below the subject's tolerance level the initial compensatory effect was clearly distinguishable. In Figure 28 retrograde eye level blood flow and momentary zero flow are exhibited on ramp up. The extent of momentary visual degradation is predictable from analysis of the flow waveform. Retrograde flow preceded visual effect while return to normal flow preceded return to full vision; in fact, the episode of flow deprivation was completed before the actual visual field decay reached peak. This observation was consistent for all subjects.

6.5.2 GOR Results

No ramp up compensatory response was noted for .1 G/sec GOR's. In all cases, retrograde blood flow preceded degradation of vision. A typical GOR response is shown in Figure 29. Retrograde blood flow began when eye level diastolic pressure decreased to 25 mmHg. Zero flow was recorded when systolic pressure decreased below 50 mmHg (mean \approx 20 mmHg). Time delay between commencement of negative mean flow and visual degradation ranged from four to



H

Figure 28. Compensatory response following rapid onset.

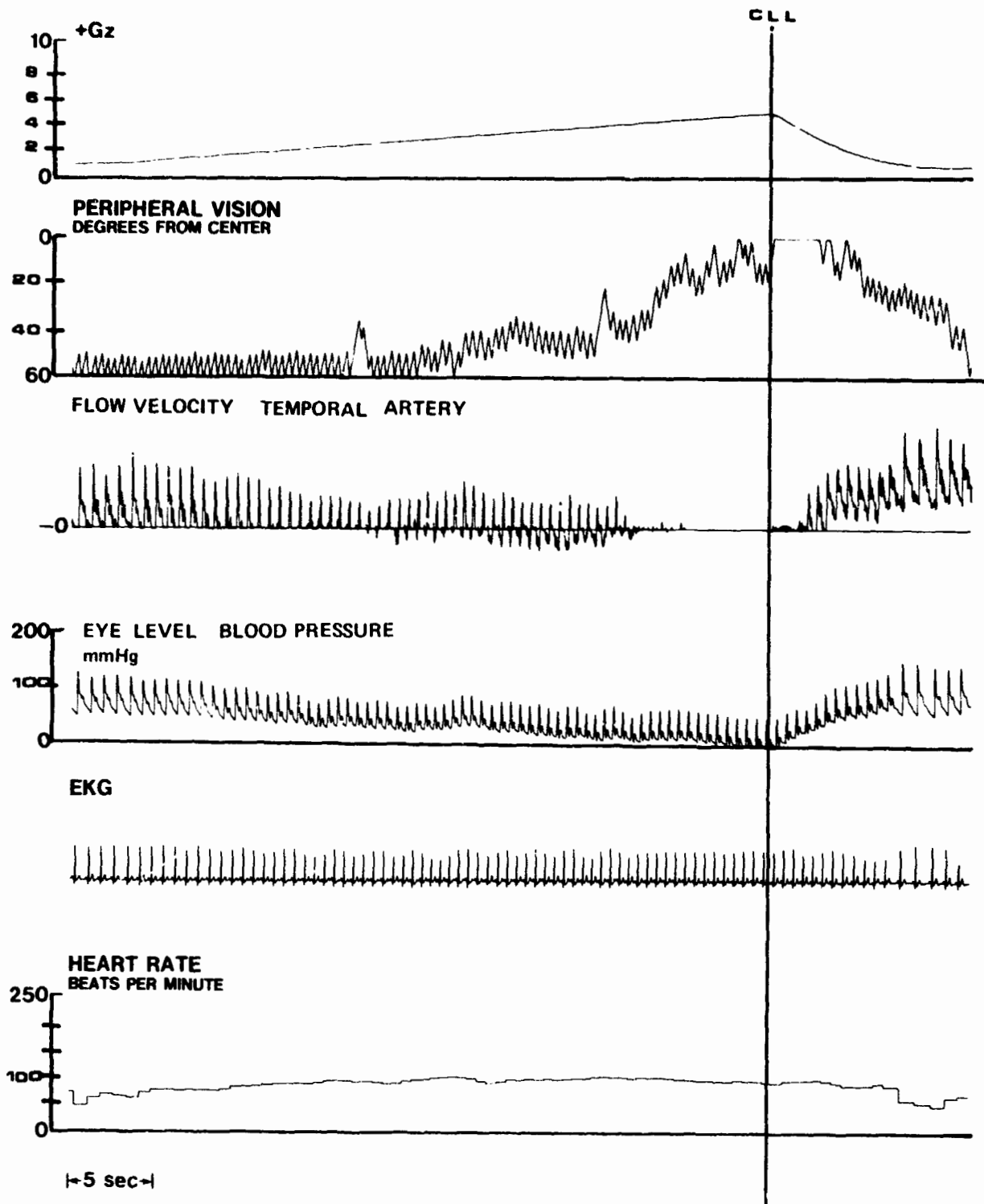


Figure 29. Correlation of visual response with blood pressure and flow velocity during gradual onset run.

eight seconds for all subjects. Time to blackout from zero flow ranged from four to nine seconds for all subjects.

6.5.3 Variable G Run Results

The temporal arterial flow signal provided, without exception, advanced indication of visual degradation. Flow velocity and direct eye level blood pressure were again observed to change synchronously thus permitting reliance on the non-invasive method rather than intrusive direct blood pressure for objective data. During the five major changes in acceleration in Figure 30, visual field change lags blood flow and pressure by several seconds. Length of time at retrograde and zero flow suggests extent of visual field change.

6.6 Applications to G Protection Technique Evaluation

During several of the previously reported experiments the subjects were asked to perform straining maneuvers at G in an effort to evaluate the use of the temporal artery flow information as an indicator of protective maneuver effectiveness. Several subjects were also asked to wear Air Force cutaway g-suits. Two types of straining maneuvers were employed. The Valsalva type, called an L-1 maneuver, consists of forcing the lungs against a closed glottis, whereas the M-1 maneuver requires a forced expiration with slow release of air (grunt). Both exercises produce an increase in thoracic pressure thereby maintaining improved cerebral circulation at high G (Shubrooks, 1973)

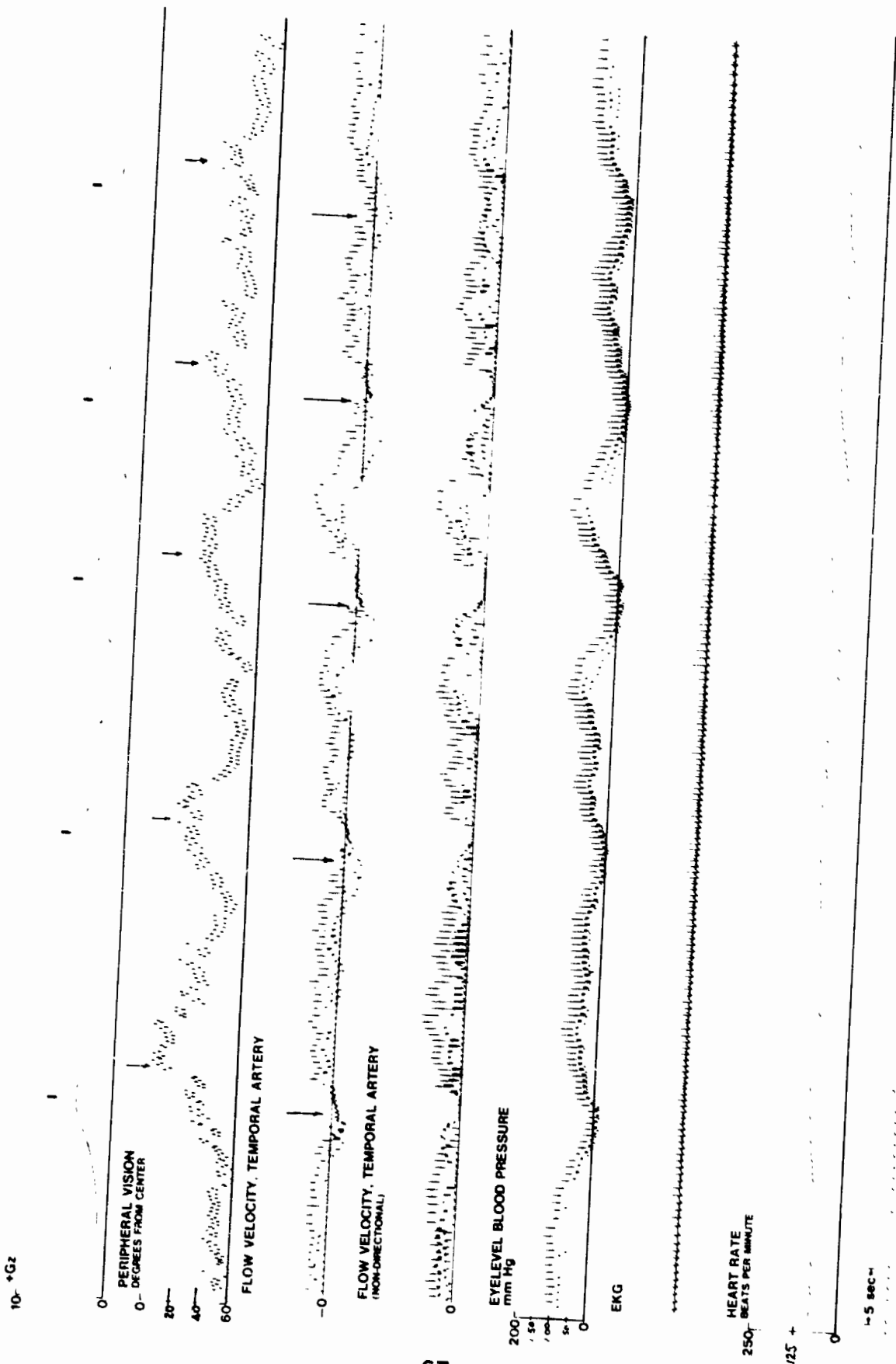


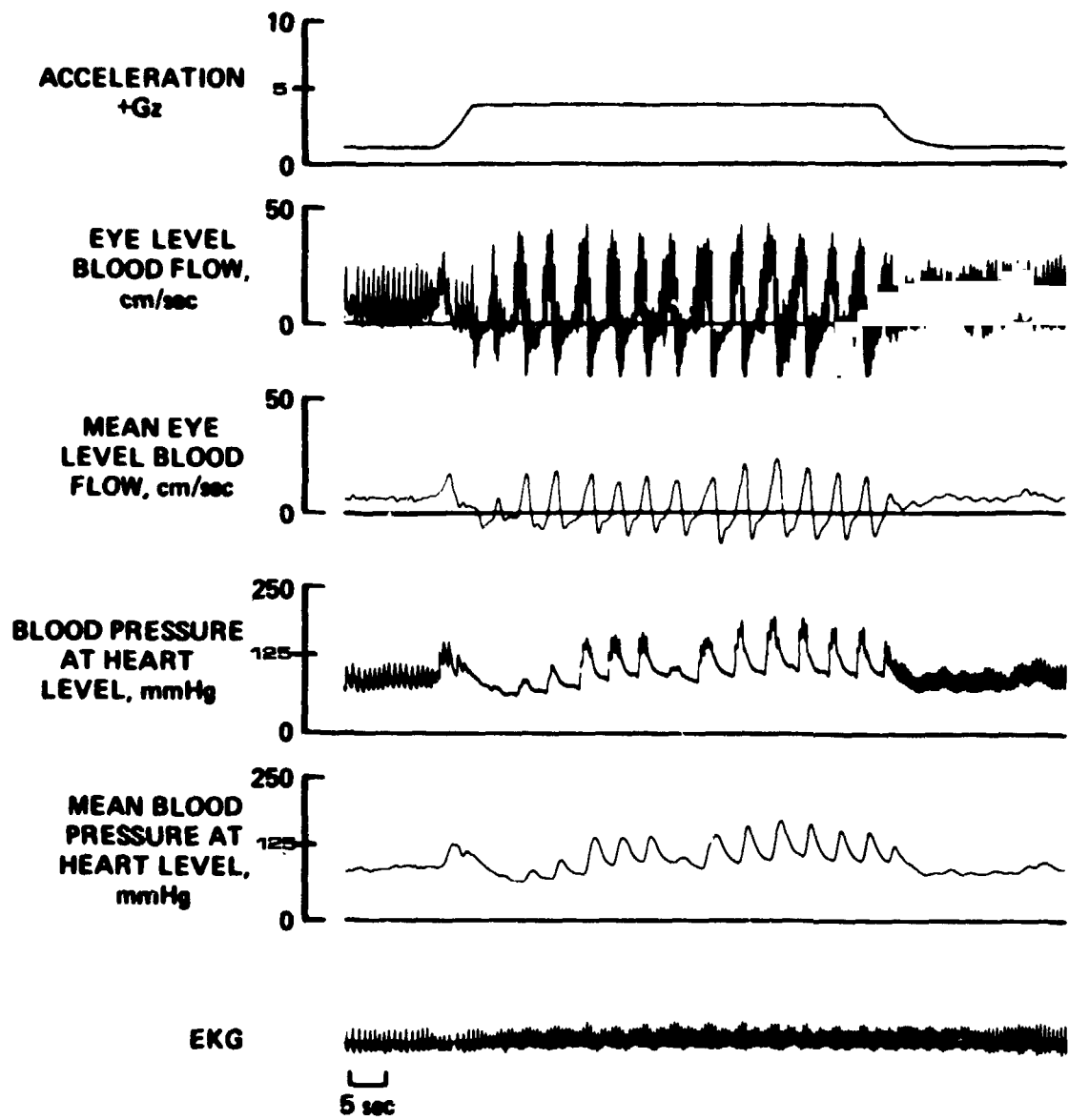
Figure 30. Correlation of visual response with eye level blood pressure and flow velocity during variable G.

Two protocols were used in an effort to gain objective evaluation of the Doppler method. For one L-1 run the subject was instructed to begin straining at the start of a run and maintain a rhythm of quick inhalation followed by a period of forcing, then quick exhalation and repeat. In another test the G protective maneuver was initiated on command of the medical monitor after objective analysis of temporal blood flow. The subject was instructed not to allow the central red light to dim beyond 50%.

6.6.1 Results - Straining Maneuvers

The Doppler information provided objective indication of cardiovascular status during the L-1 maneuvers and the g-suit inflations; however, the grunting noise of the M-1 produced interference in the Doppler information. Vibrations of the skull during loud vocal outbursts are sensed as motion by the Doppler probe and because little tissue exists below the temporal artery, there is little attenuation of skull vibrations. An operator with a trained ear can detect the characteristic changes in flow patterns; however, the Doppler electronics used for these tests can not easily discriminate between voice and blood flow.

Results of an L-1 maneuver are shown in Figure 31. The G level chosen for this subject was 0.7 G higher than his normal tolerance - he would have easily blacked out without the L-1.



SUBJECT: J. C. W.

Figure 31. Response to L-1 maneuver during rapid onset run.

Heart level blood pressure reflects the increased intrathoracic pressure during the first strain on ramp up. Blood flow parallels the blood pressure signals, rhythmically increasing during strain and shows significant retrograde activity during exhalation and inhalation phases. Commenting on the condition of his vision during the run, the subject reported "my lights kept going in and out." He reported an apparent time lag between increased lung pressure and visual field return, thus supporting the previous findings with the Gillingham light bar reported in Section 6.5.

Poor performances of the L-1 technique by some subjects were consistently recognized by abnormally long periods of retrograde or zero flow while the subject took too long to take in a new breath.

6.6.2 Results - G-Suit

Effect of g-suit inflation on temporal arterial blood flow is shown in Figure 32. Non-directional blood flow is compared with g-suit pressure. As seen in the figures at (a) retrograde flow begins late in diastole as the G force increases in a 0.1 g/sec GOR. When the g-suit is suddenly pressurized at (b) retrograde flow disappears, signalling the arrival of more blood from the lower extremities and increased eye level blood pressure. As the G force continues to increase retrograde flow resumes at (c), however, at a later time than if no g-suit had been used.

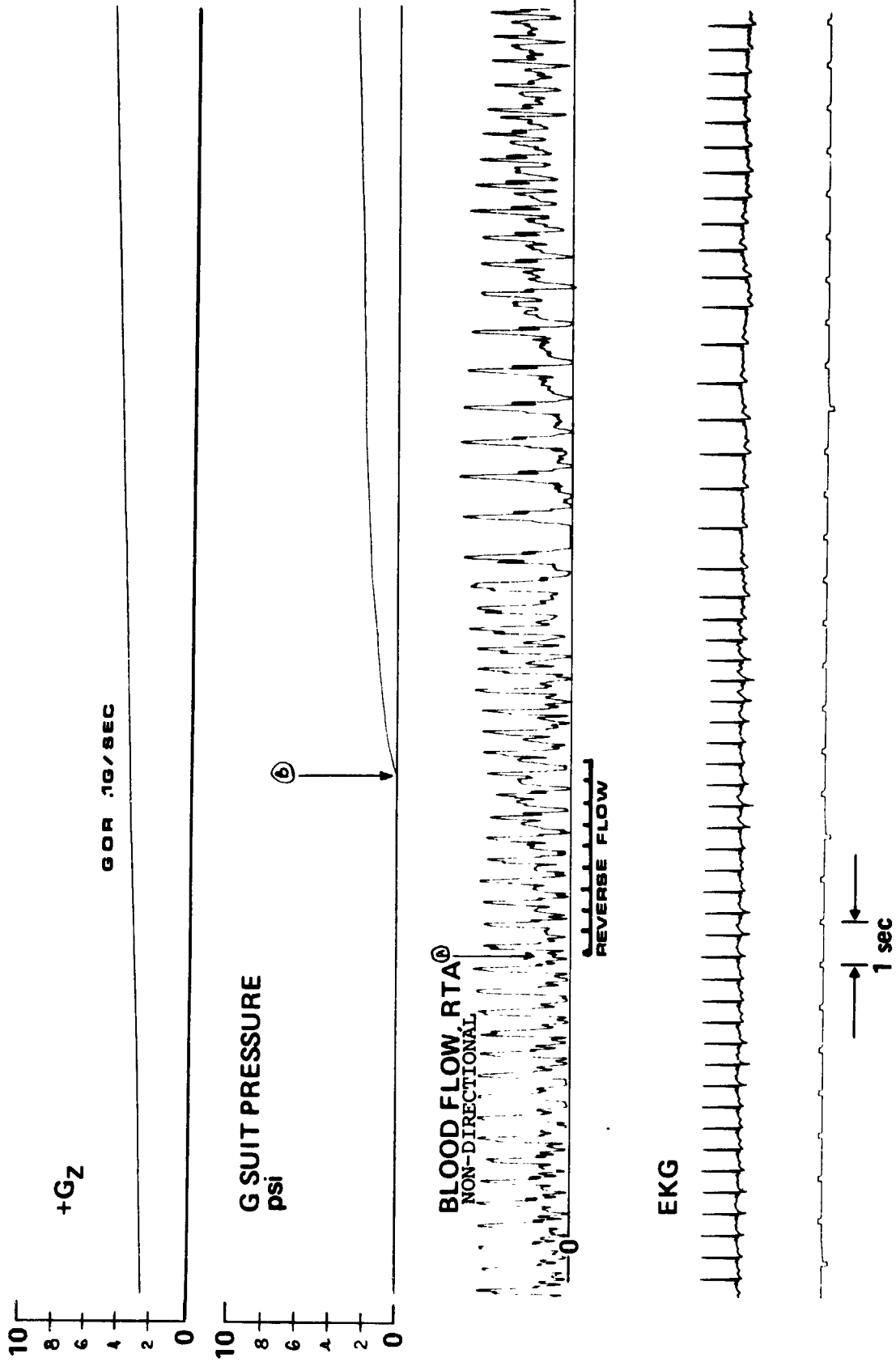


Figure 32. G-suit inflation modifies eye level blood flow velocity.

An objective comparison of g-suit and L-1 effectiveness with unassisted (relaxed) runs is shown in Figure 33. Run 1 was terminated by the subject at 50% CLL. Note that temporal Doppler shows the same objective end point. During Run 2 the medical monitor activated g-suit pressure upon objective evaluation of Doppler signals. Blood flow immediately resumes and maintains an unaltered peak velocity until the run was automatically terminated at 6.9 G. (The respiration induced changes in flow seen before inflation are not present during the g-suit activation.) The subject reported 25% CLL at time of g-suit activation with return of full vision within three seconds. Upon objective analysis of flow signals in Run 3 the subject was asked to begin an L-1. Immediate return of flow is noted followed by the characteristic flow changes observed earlier in Figure 31. As 7 G approached the subject had difficulty maintaining his straining effectiveness as evidenced by diminished flow amplitude and longer periods of zero flow. The subject reported periodic alterations in visual field during the last part of the run.

6.6.3 Results - Tilt-Back Seat

Temporal artery blood flow accurately predicted visual degradation for all subjects at all three seat-back angles (13°, 45°, 65°). All subjects reached protocol maximum of 7.0 G at the 65° back angle without visual failure or flow cessation. Typical

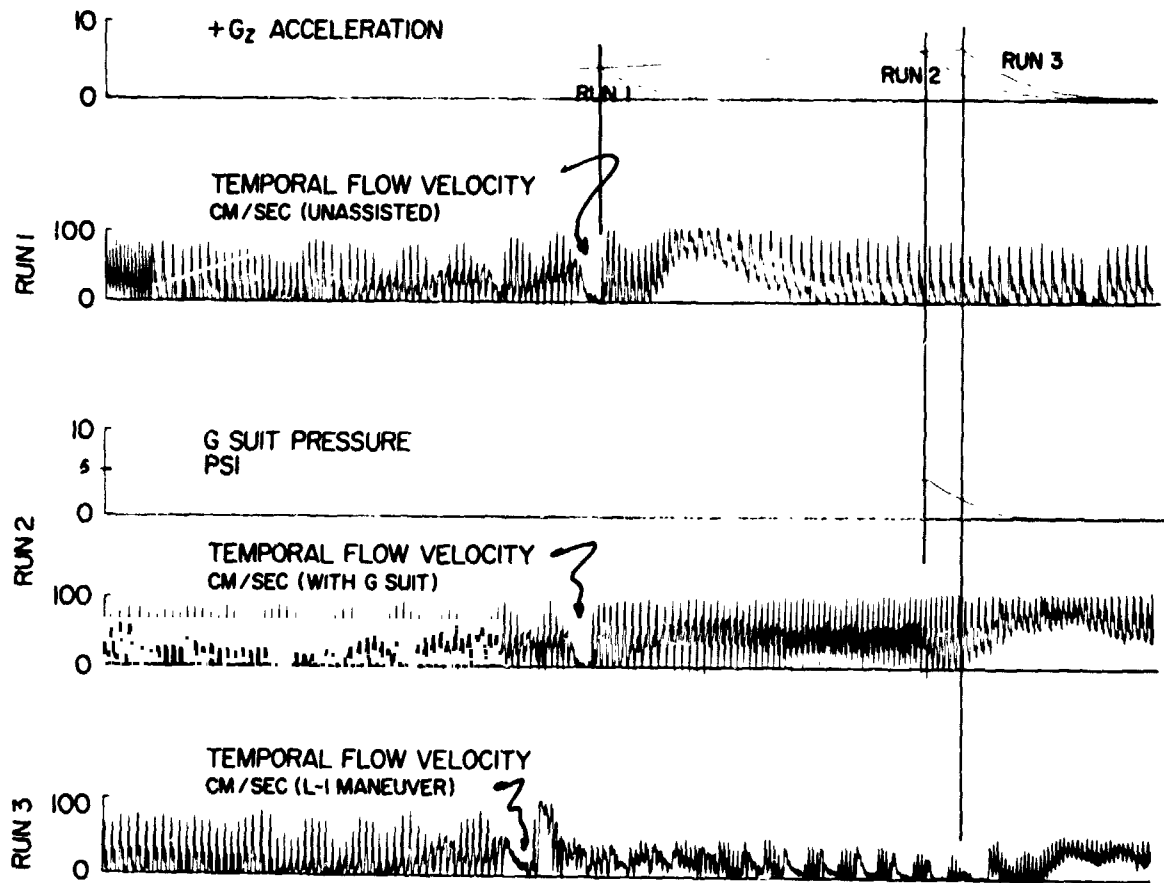


Figure 33. Cardiovascular response to protective maneuvers (g-suit and L-1 initiated upon analysis of temporal flow velocity).

results for 13°, 45° and 65° are presented in Figures 34, 35 and 36 respectively. At 13° blood flow ceased three seconds before onset of final visual field change and seven seconds before blackout at 5.9 G. Consistent diastolic flow reversal began at 2.6 G. At 45° the run terminated at 6.2 G after 4.5 seconds of zero flow. Visual field rapidly decayed beginning 5.5 seconds after zero flow even though centrifuge was decelerating. Duration of maximum vision loss was minimized by return of forward flow and reduced G load. Retrograde diastolic flow began at 3.2 G. At the 65° back angle peak velocities at systole remained fairly constant throughout the run with no visual end point or major change in vision reported by subject. Reverse flow began at 4.2 G.

6.7 Safety

During the more than 1000 runs at NASA-Ames and over 300 runs at USAFSAM no subject reached unconsciousness without a period of at least 13 (range 13 to 23) seconds of negative mean or zero flow. The flowmeter also acted as a good backup to EKG as a safety monitoring device.

EKG and heart rate signals recorded during the rapid onset run in Figure 37 do not reveal that the heart was pumping at one-half the EKG rate as seen in the flow recording. The condition, pulsus alternans, was even more evident in subsequent GOR and GOG

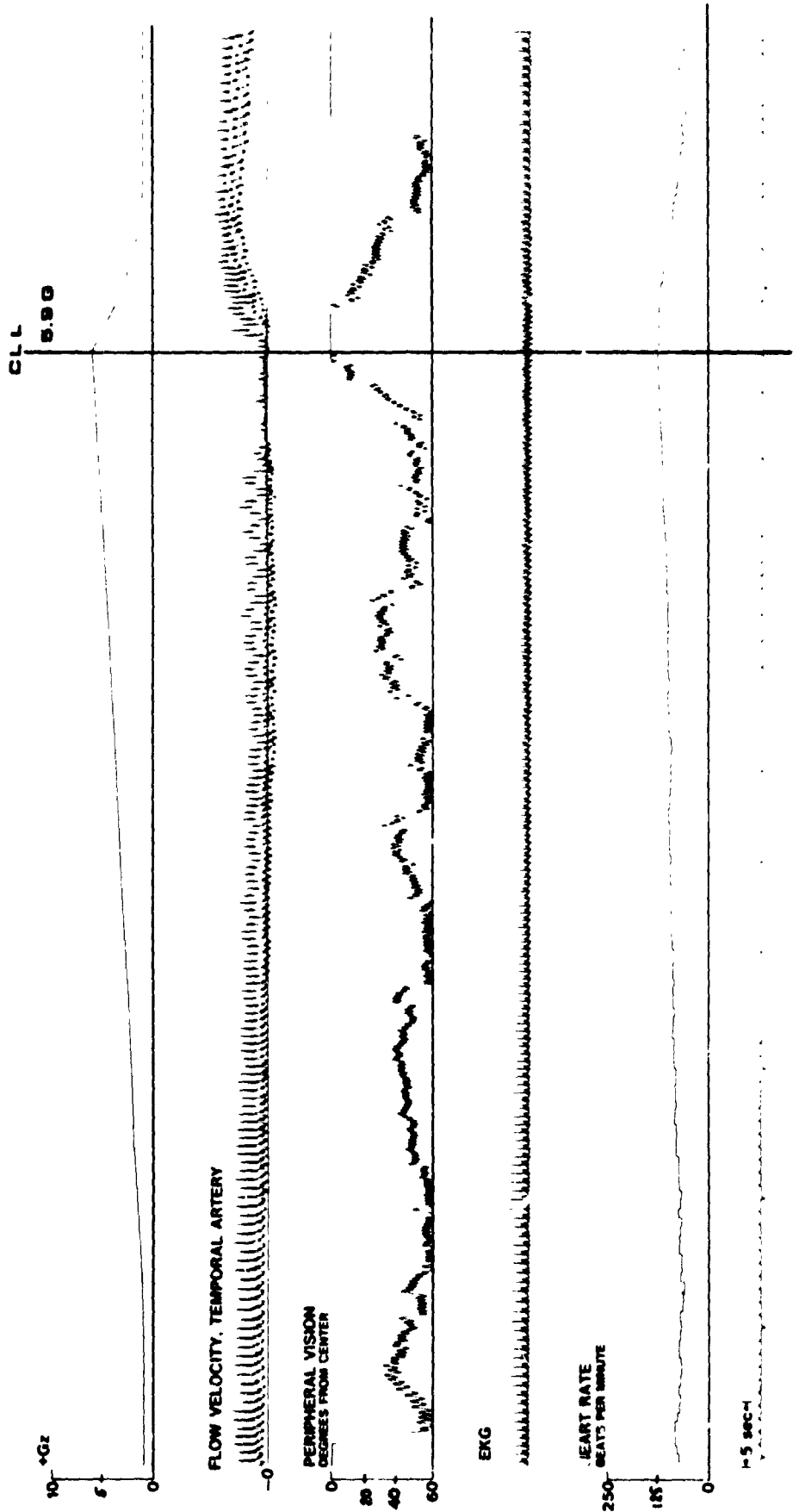


Figure 34. Response to 130° tilt back seat.

M

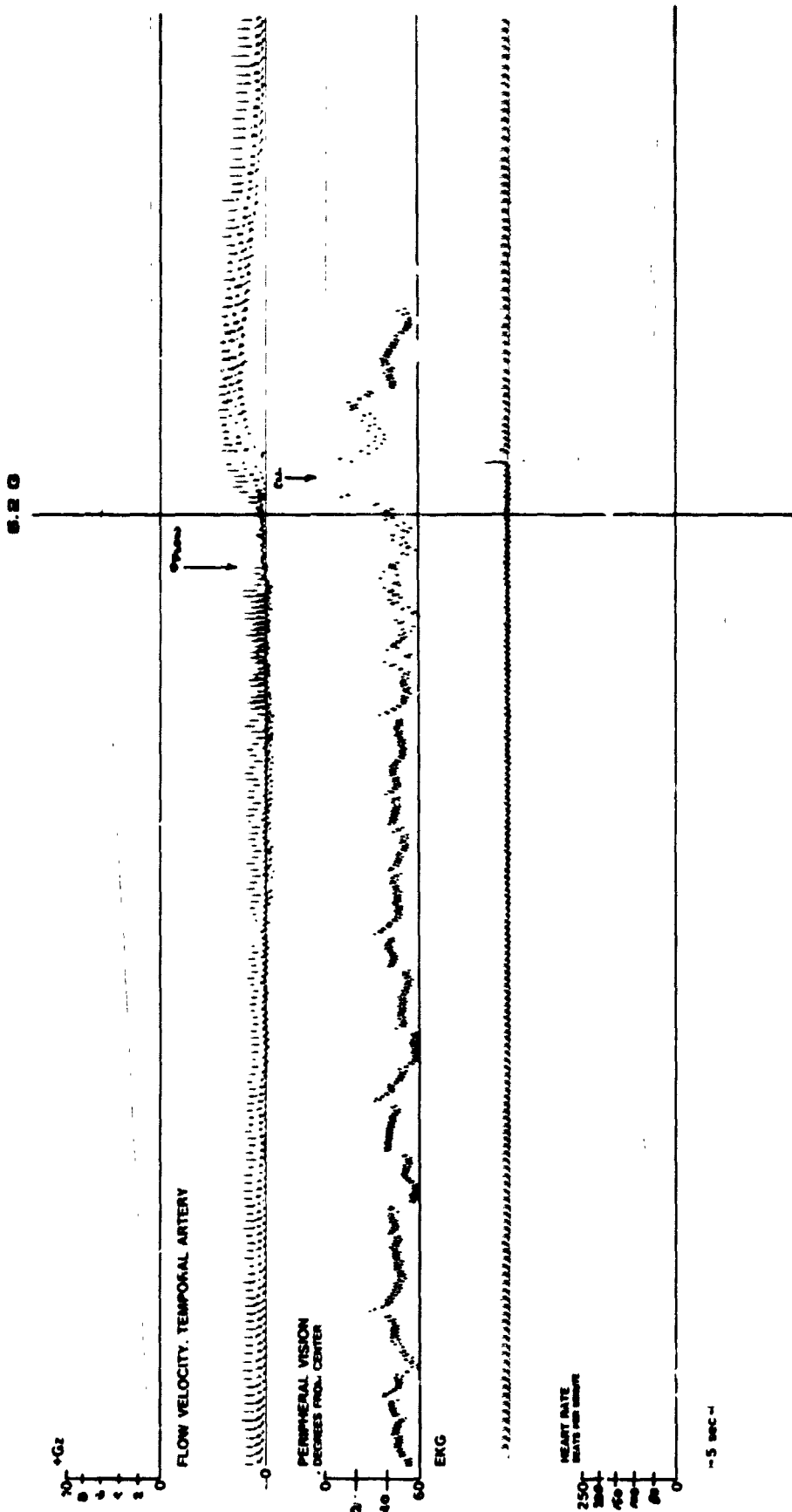
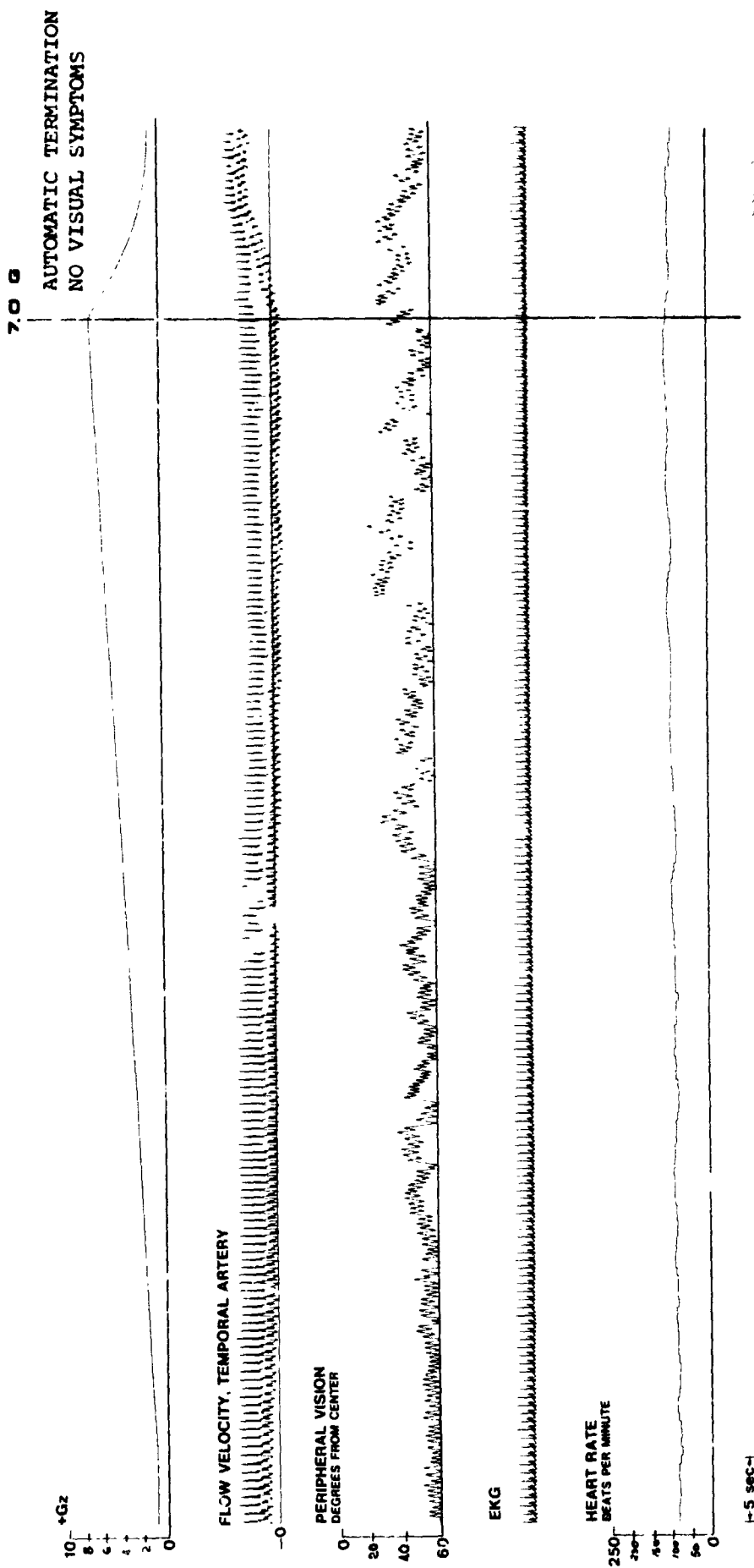


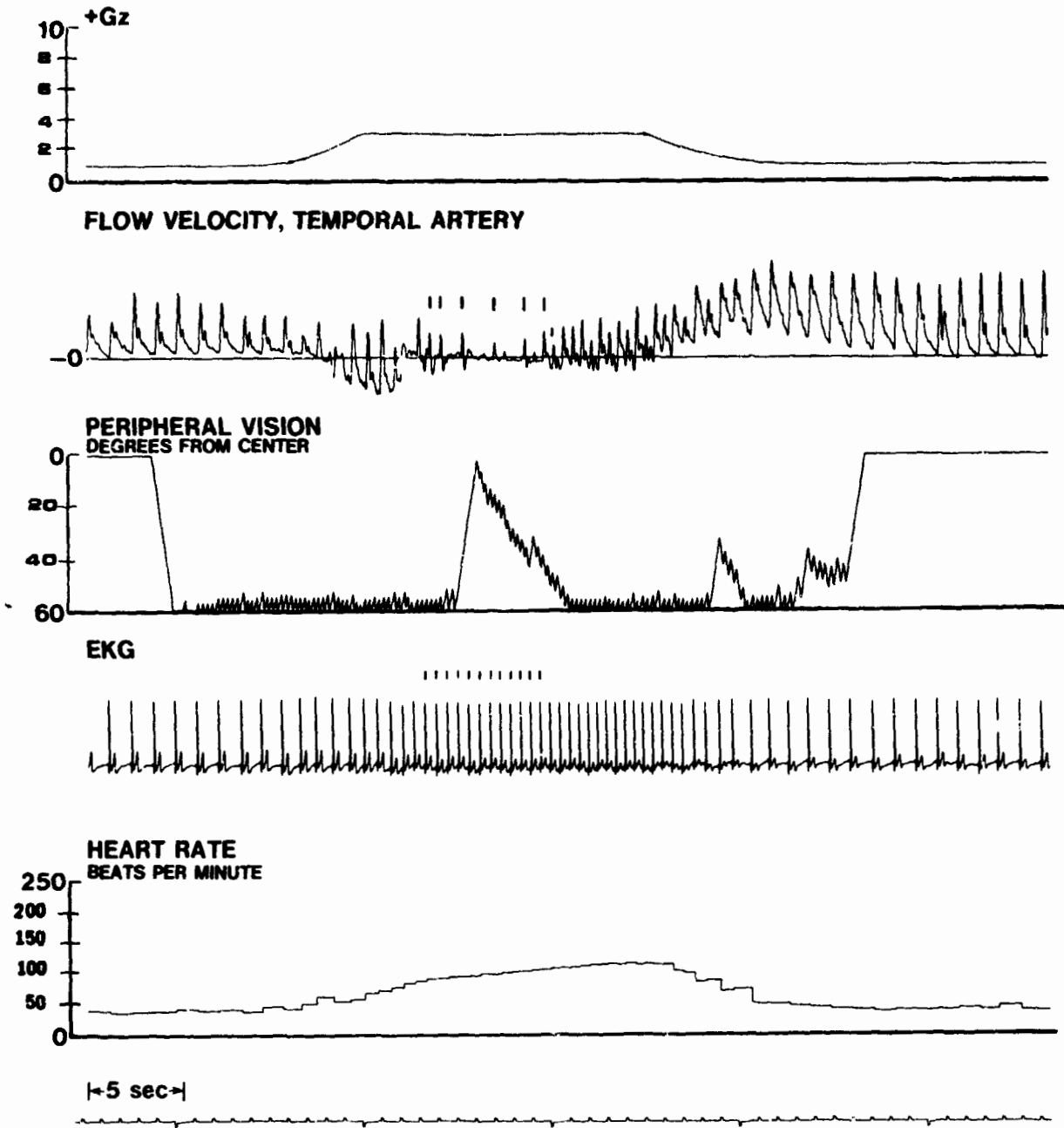
Figure 35. Response to 45° tilt back seat



H

Figure 36. Response to 65° tilt back seat

runs. EKG record for the GOR, Figure 38, shows an initial alteration in rate at start of run; however, nothing in EKG for heart rate could explain the alternating visual field experienced between 2 G and visual end point. Reference to the blood flow waveform explains the problem - a relatively weak flow signal at one-half the EKG rate. During the variable G run, Figure 39, flow is present only every other EKG pulse. Reliance on the EKG alone would not have revealed this physiological condition.



CO

Figure 37. Temporal blood flow recording reveals nulsus alternans during rapid onset run

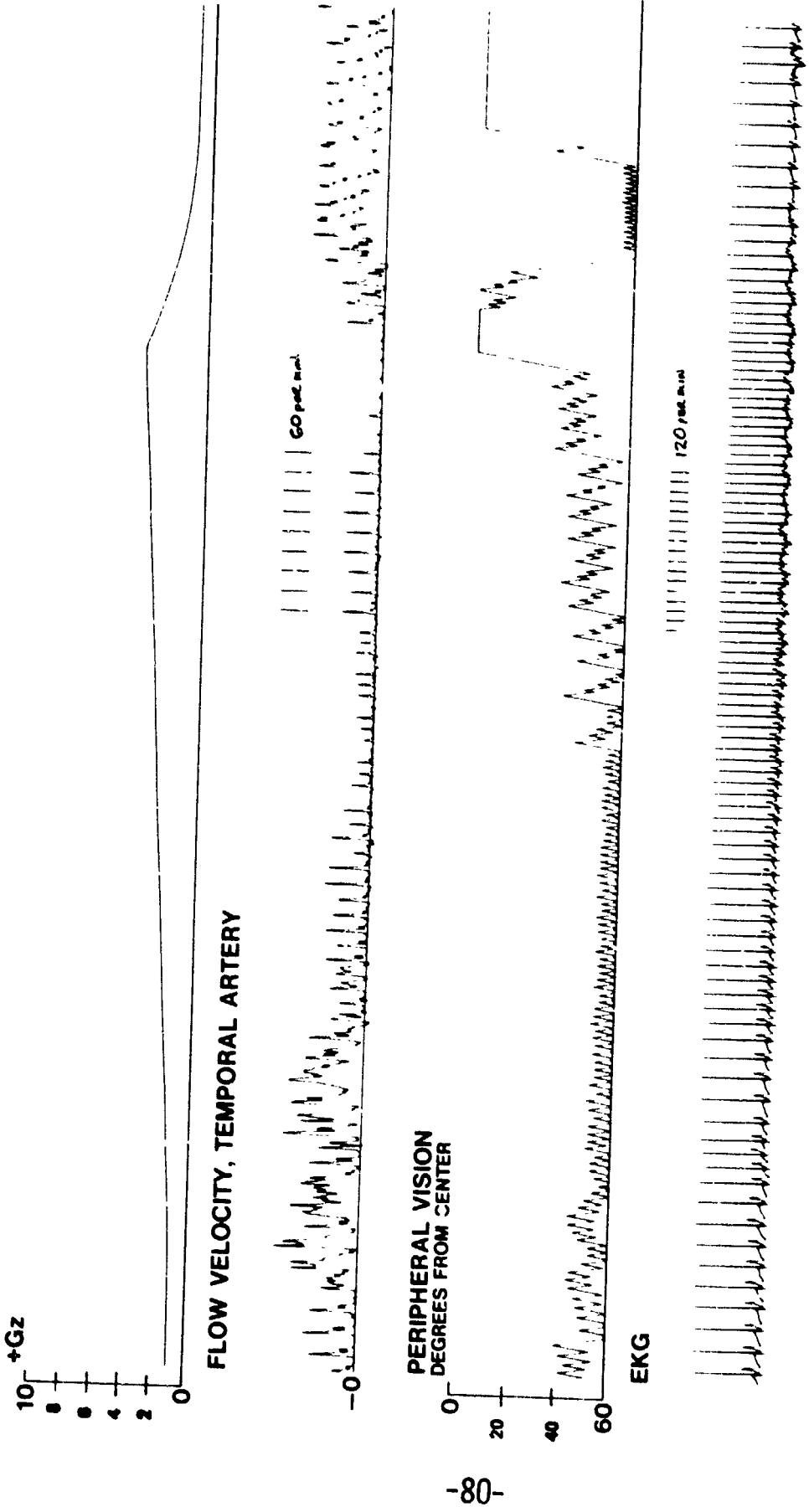


Figure 38. Temporal blood flow recording reveals pulsus alternans during gradual onset run

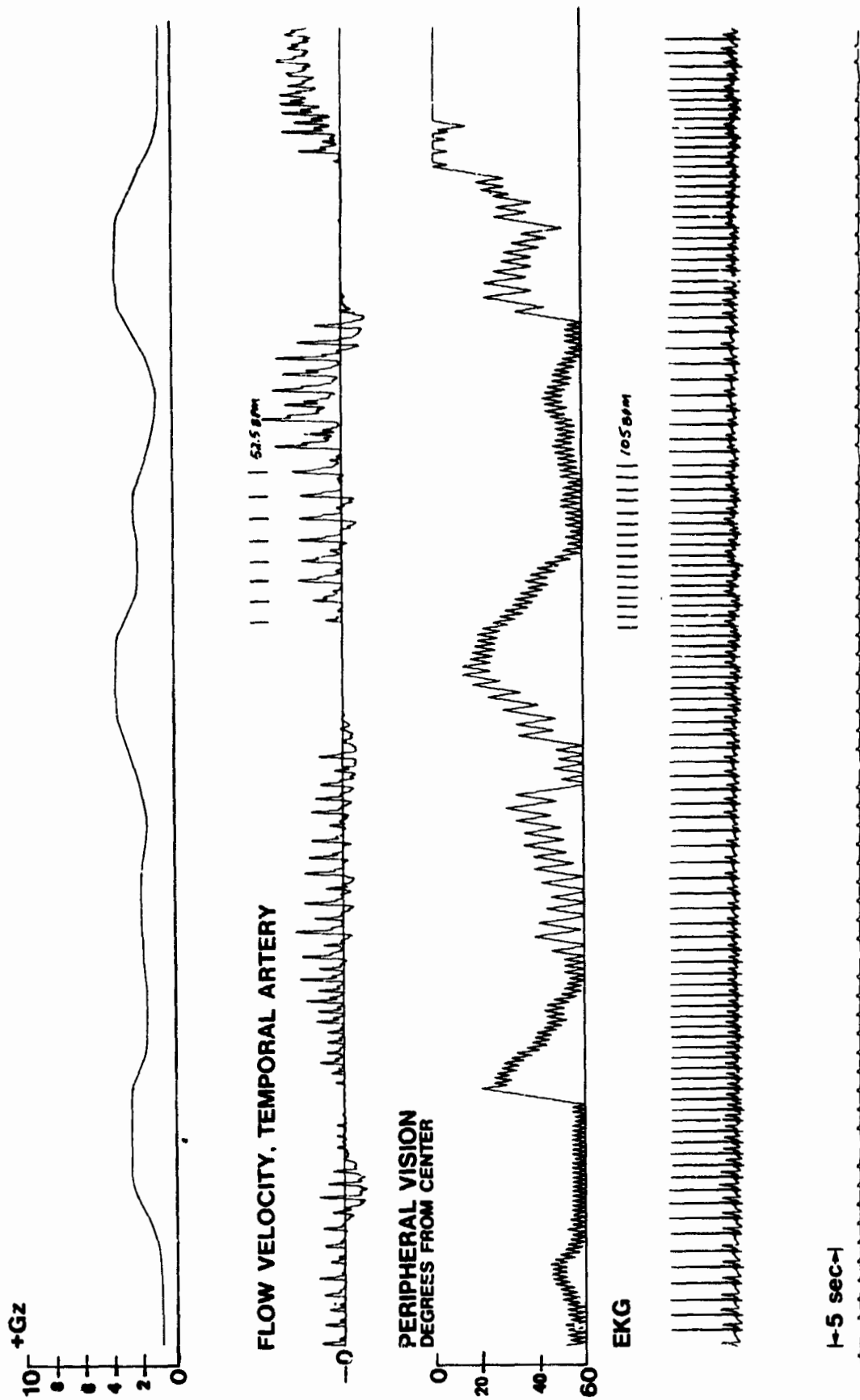


Figure 39. Temporal blood flow recording reveals pulsus alternans during variable G run

7.0 DISCUSSION

7.1 Correlation with Direct Eye Level Blood Pressure

The objectivity of the new method was supported in each experiment. Eye level blood pressure and temporal artery flow velocity during rapid onset, gradual onset and variable G profiles consistently indicated objective end points. Good correlation between flow velocity and pressure shows that the vessel resistance change is not significant during +G_z. Start of retrograde flow coincided with a drop in diastolic pressure below 25 ±5 mmHg. Although eye-heart distance was not measured for these subjects, a negative pressure gradient in diastole can be hypothesized. Assuming a nominal 33 cm eye to heart distance and 80 mmHg diastolic pressure, reverse pressure gradient would exist above 3.3 G (at 3.3 G a 33 cm column of blood produces a back pressure on the heart of 80 mmHg). Rushmer suggested that a lower cerebral spinal fluid pressure provided a siphon effect to maintain a positive pressure gradient to help maintain cerebral perfusion. Results using the carotid flow probe tend to support Rushmer's hypothesis. Carotid flow exhibited retrograde flow only during the period of maximum reversal in the temporal artery; however, forward carotid flow resumed very quickly while the temporal flow ceased. The carotid artery appeared to be influenced by a lower pressure in the cerebral bed, as measured by Rushmer, while the external artery was

more influenced by hydrostatic pressures. Explanation of the good correlation between retinal artery flow and temporal artery flow is more difficult. Retrograde flow and flow cessation in retinal blood vessels as previously described by Duane (1954) and Leverett (1971) coincides with these findings in the temporal artery. Several branches of the ophthalmic and superficial temporal arteries are in close proximity as seen in Figure 40. Several branches of the superficial temporal artery do anastomose with the lacrimal and supraorbital branches of the ophthalmic artery. This suggests some hydrostatic commonality between retinal and temporal arteries.

The retinal artery observations of Duane and Leverett supported the early hypothesis of Andina that blackout was caused by exsanguination of the retinal artery when eye level pressure became less than intraocular pressure. That intraocular pressure is the sole cause of flow cessation at 20 mmHg cannot be supported by the findings of this work. Flow in the superficial temporal artery also ceases at 20 mmHg. It is doubtful that intraocular pressure in excess of retinal arterial pressure, even in the presence of anastomosis, could have significant effect on superficial pressure in the temporal artery. The cessation of forward flow is, therefore, assumed to be related to attainment of critical closing pressures of branches of the temporal artery (Nichol, 1951).

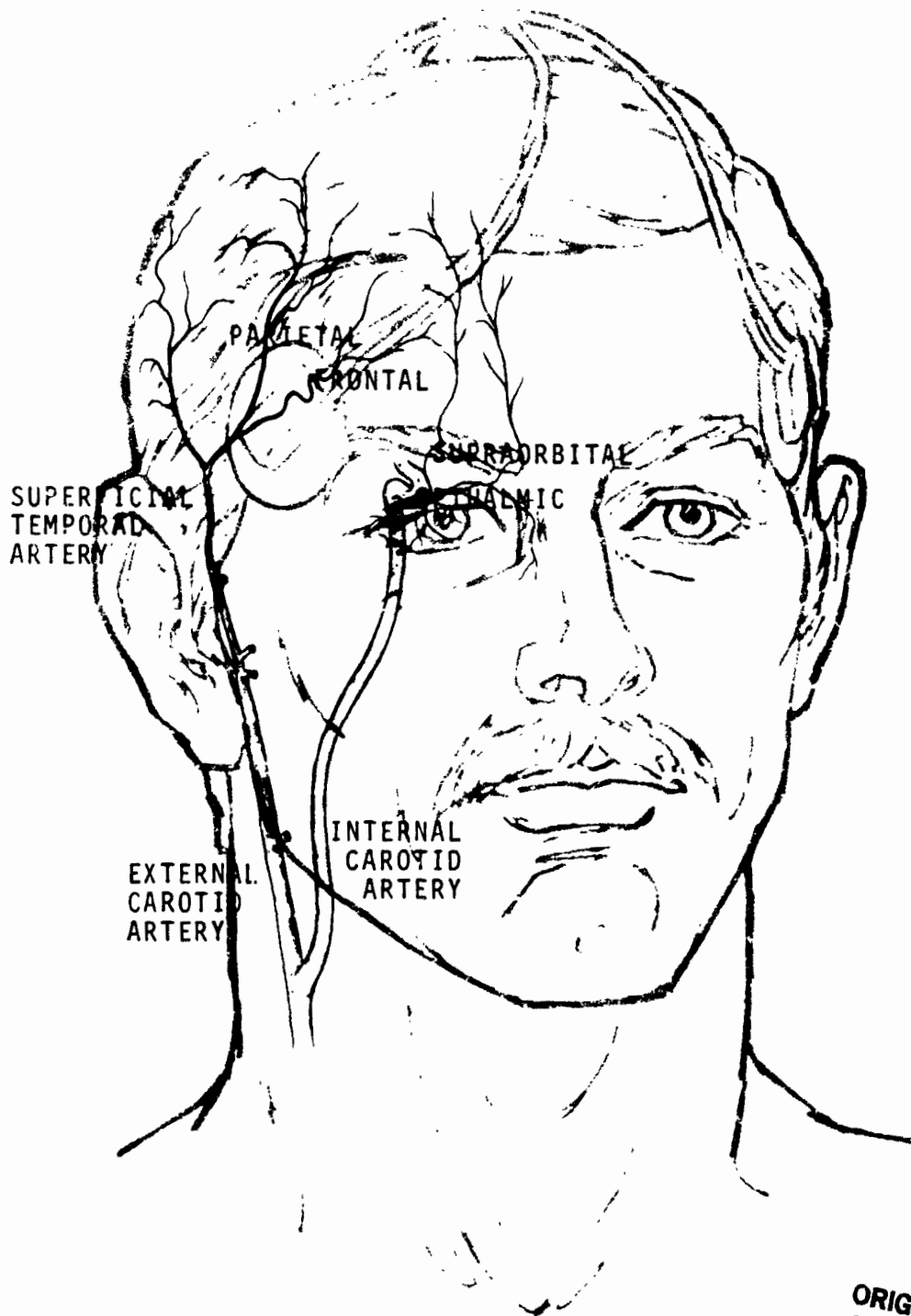


Figure 40. Proximity of branches of the temporal and ophthalmic arteries.

ORIGINAL PAGE IS
OF POOR QUALITY

7.2 Correlation with Visual End Points

In the experiments at Ames Research Center using inexperienced subjects, twenty percent of the subjects reported end points which did not coincide with blood flow data. The experiments at USAFSAM suggested that inexperience, fear, boredom, etc. were causes for discrepancy at Ames. Even some experienced subjects reported early end points in the gradual onset profiles as reported in Section 6.3. However, when the medical monitor determined the end points for these same subjects in a subsequent run - based objectively on Doppler flow data - all subjects reported agreement with the objective end point. Because no subject became unconscious or reported visual degradation beyond 60% CLL it was concluded that the Doppler method could be used as an objective end point criterion.

Eye level blood flow response to ROR indicated cardiovascular compensation time to G-induced increase in hydrostatic pressure is three to five seconds. If the plateau G level after a rapid onset is sufficient to cause a net negative or zero flow for four to seven seconds, blackout will occur before the system compensates by supplying oxygenated blood to the retinal artery. During GOR this compensatory response is avoided thus permitting higher G acceleration levels to produce blackout. This observation suggests that each subject may have an optimal onset rate; however, data to support this hypothesis was not obtained.

The Gillingham light bar provided the most definitive correlation of visual and cardiovascular deterioration. Eye level flow changes always preceded the onset of visual field change. Some subjects detected the existence of flashing peripheral lights even after experiencing a diminished center red light. Flow data for these subjects supported the loss of central vision. Sensitivity to a flashing stimulus after diminished central vision suggests that thought be given to light intensity of the flashing stimuli.

7.3 Comparison to Ear Opacity End Points

Reports on the photoelectric ear opacity end point technique indicate good concurrence with blackout. Of all the noninvasive methods reviewed, ear opacity measurement most closely compares with the new temporal artery Doppler technique. Flow reversal was found to be a highly significant precursor to cardiovascular deterioration in this study, however, the ear pulse, derived photometrically, cannot reveal flow reversal. An experiment to establish the relationship of flow in the external vessels of the ear to temporal artery flow would be desirable. Results of this study indicate that presence of reversal in diastole, which is easily distinguished in both the graphic and audio recordings, provides important warning of impending visual failure.

7.4 Limitations

Application of the Doppler probe requires some skill and patience. Care must be taken to obtain an optimal flow signal before fixing the device on the skin. Poor transmission of the ultrasonic beam created by insufficient use of gel or air entrapment will produce poor results. Heavy sweating may cause the taped-on sensor to come loose. Two hours seemed to be a reasonable time to expect good adherence in the centrifuge environment. In high noise environments or during an M-1 maneuver, additional frequency components are sensed and included in the output signal. Use in a jet aircraft cockpit would be limited by current electronics technology. The method is qualitative rather than quantitative because blood vessel diameter is not determined. Since it is not expected that the temporal artery would constrict in the hypoxic conditions of this stress, flow velocity is probably a good analog of flow.

Application to other operational situations such as L-1 maneuver, g-suit, and tilt-back seat in addition to the more common relaxed centrifuge runs has been adequately explored in this study to recommend its use as an objective tolerance measurement technique. If adequate safeguard to blackout or reentry during shuttle cannot be guaranteed, this sensor should be evaluated for use as a safety monitoring procedure.

8.0 CONCLUSIONS

The transcutaneous Doppler ultrasonic flowmeter monitoring temporal artery blood flow velocity appears to be a reliable technique for measuring cardiovascular status and predicting visual failure during +Gz acceleration. Cardiovascular status as indicated by eye level blood pressure has been well correlated with changes in eye level blood flow and objective visual changes reported by experienced centrifuge subjects. Visual changes effected by +Gz acceleration were consistently preceded by easily recognizable changes in the graphic and audio recordings from the Doppler flowmeter. Diastolic retrograde flow leading to negative mean flow and eventual cessation provide graphic clues several seconds prior to visual degradation and failure. The accompanying audio signal changes are distinctive and serve to warn the medical monitor that cardiovascular status is deteriorating.

The method has been successfully demonstrated during rapid onset, gradual onset, and variable G stress. It has further provided an objective indication of G tolerance during L-1 maneuvers, g-suit inflation and evaluation of altered seat back angles.

The objective nature of the method further suggests its use during G tolerance tests involving tracking tasks or other activities requiring visual attention. It should also be considered as a safety monitoring procedure during reentry if there is doubt about a space passenger's cardiovascular status.

9.0 REFERENCES

- Andina, F.: "Schwarzsehen als Ausdruck von Blutdruckschwankungen bei Sturzfliegen. Schweiz. Med. Wchnschr., 67:753-756 1937.
- Browne, M.K.; Fitzsimmon, J. T.: Electrocardiographic Changes during Positive Acceleration. FPRC-1009, 1957.
- Burton, A.C.: Hemodynamics and the Physics of the Circulation. T. C. Ruch and J. F. Fulton (eds.), Medical Physiology and Biophysics, W. B. Saunders Co., 1960.
- Chambers, R.M.: Long Term Acceleration and Centrifuge Simulation Studies. Aviation Medical Acceleration Laboratory, 1963.
- Coburn, K. R.: Physiological End Points in Acceleration Research. *Aerospace Med.* 41:5-11, 1970.
- Duane, T. D.: Observations on the Fundus Oculi During Blackout. *A.M.A. Arch. Ophthal.* 51:343, 1954.
- Duane, T. D.; Lewis, D. H.; Weeks, S. D.; Toole, J. F.: The Effects of Applied Ocular Pressure and of Positive Acceleration on Photic Driving in Man. NADC-MA-6214, 1962.
- Flax, S. W.; Webster, J. C.; Updike, S. J.: Statistical Evaluation of the Doppler Ultrasonic Flowmeter. *Biomedical Sciences Instrumentation*. Plenum Press, New York, p. 201-222, 1970.
- Franklin, D. L.; Schlegel, W. A.; Rushmer, R. F.: Blood Flow Measured by Doppler Frequency Shift of Backscattered Ultrasound. *Science* 134:564-565, 1961.
- Fraser, T. M.: Human Response to Sustained Acceleration. NASA SP-103, 1966.
- Greenleaf, J. E.; van Beaumont, W.; Bernauer, E. M.; Haines, R. F.; Sandler, H.; Staley, R. W.; Young, H. L.; Yusken, J. W.; Effects of Rehydration on +G_z Tolerance After 14 Days Bed Rest. *Aerospace Med.* 44(7):715-722, 1973.
- Kalmus, H. P.: Direction Sensitive Doppler Device. *Proc. IRE* p. 698, 1955.
- Lambert, E. I.; Wood, E. H.: Direct Determination of Man's Blood Pressure on the Human Centrifuge During Positive Acceleration. *Fed. Proc.* 5:59, 1946.

- Lambert, E. H.: The Physiologic Basis of "Blackout" as it Occurs in Aviators. Fed. Proc. 4:43, 1945.
- Leverett, S. D., Jr.; Newson, W. A.: Photographic Observations of the Human Fundus Oculi During +G_z Blackout on the USAF School of Aerospace Medicine Centrifuge. In Lunc, M. (ed). XIXth International Astronautical Congress Bioastronautics - Book 4. Oxford: Pergamon, p. 75-79, 1971.
- Leverett, S.D.; Shubrooks, S. J.; Shumate, W.: Some Effects of Space Shuttle +G_z Reentry Profiles on Human Subjects. Proc. Aerosp. Med. Mtg., p. 90, 1971.
- Leverett, S. D.; Whitney, R. U.; Zuidema, G. D.: Protective Devices Against Acceleration. In O. H. Gauer and G. D. Zuidema (eds.), Gravitational Stress in Aerospace Medicine, Little, Brown and Co., Boston, 1961.
- Lindberg, E. F.; Wood, E. H.: Acceleration. In J. H. Brown (ed.), Physiology of Man in Space. Academic Press, New York, 1963.
- Mancini, R. E.; Rositano, S. A.; Luzzi, E. P.; Sandler, H.: Doppler Blood Flow Systems for Chronic Animal and Human Use. 26th ACEMB Minneapolis, 1973.
- McGuire, T. F.; Marshall, H. W.; Nolan, A. C.; Lindberg, E. F.; Wood, E. H.: Comparison of Changes in Arterial Oxygen Saturation During Transverse Acceleration as Indicated by Ear Oximetry and by Direct Photometry on Arterial Blood. Proc. 32nd Aerosp. Med. Assoc., 1961.
- McLeod, F. D., Jr.: Doppler Blood Flowmeter, In Progress Report on NASA Grant NRG 33-01C-074, p. 4-7, 1969.
- McLeod, F. D., Jr.: A Directional Doppler Flowmeter. Digest of Seventh International Conference on Medical and Biological Engineering, Stockholm p. 213, 1967.
- Olson, R. M.; Cook, J. P.: Human Carotid Artery Dimension and Blood Flow by Noninvasive Technique. Medical/Instrumentation, Vol. 7 #1, p. 70-71, Jan/Feb 1973.
- Rositano, S. A.; Sandler, H.: Multichannel Doppler Blood Flow Measurement System. 8th International Conference on Medical and Biological Engineering, Chicago, 1969.

- Rositano, S. A.; Luzzi, E. P.; Mancini, R. E.; Sandler, H.: A Multichannel Directional Doppler Flowmeter. 26th ACEMB, Minneapolis, 1973.
- Rositano, S. A.; Mancini, R. E.; et al: Noninvasive Determination of Human Tolerance to +G_z Acceleration. 25th ACEMB, p. 440, 1972.
- Rushmer, R. F.; Baker, D. W.; Stegal, H. F.: Transcutaneous Doppler Flow Detection as a Non-destructive Technique. J. Appl. Physiol. 21:554, 1966.
- Ryan, J. F.; Raines, J.; Dalton, B. C.; Mathieu, A.: Arterial Dynamics of Radial Artery Cannulation. Anesth. Analg. Curr. Res. 52:1017-1025, 1973.
- Samaan, H. A.: The Hazards of Radial Artery Pressure Monitoring. J. Cardiovascular Surg. 12:342, 1971.
- Satomura, S.: Ultrasonic Doppler Method for Inspection of Cardiac Functions. Journal of Acoustical Society of America, 29, p. 1181, 1957.
- Satomura, S.; Kanedo, A.: Ultrasonic Blood Rheograph. Third International Conference on Medical Engineering, p. 254-258, 1960.
- Sem-Jacobsen, C. W.: Recording of In-flight Stress in Jet Fighter Planes. Aerosp. Med., 31:320, 1960
- Shubrooks, S. J., Jr.; Leverett, S. D., Jr.: Effect of the Valsalva Maneuver on Tolerance to +G_z Acceleration. J. Appl. Physiol. 34:460.466, 1973
- Smedal, H. A.; Rogers, T. A.; Duane, T. D.; Holden, G. R.; Smith, J. R.: The Physiological Limitations of Performance During Acceleration. Aerosp. Med., 34:48, 1963.
- Squires, R. D.; Jensen, R. E.; Sipple, W. C.; Gordon, J. J.: Electroencephalographic Changes in Human Subjects During Blackout Produced by Positive Acceleration. NADC-MA-6402, 1964.
- Stegal, H. F.; Rushmer, R. F.; Baker, D. W.: A Transcutaneous Ultrasonic Blood-Velocity Meter. J. Appl. Physiol. 21(2): 607-711, 1966.

Wood, E. H.; Lindberg, E. F.; Code, C. F.; Baldes, E. J.:
Photoelectric Earpiece Recordings and Other Physiologic Variables as Objective Methods of Measuring the Increase in Tolerance to Headward Acceleration (+G_z) Produced by Partial Immersion in Water. WADD-AMRL-TDR-63-106, 1963.

Wood, E. H.; Lambert, E. H.; Baldes, E. J.; Code, C. F.: Effects of Acceleration in Relation to Aviation. Fed. Proc., 5:327, 1946.

Wood, E. H.; Nolan, A. C.; Donald, D. E.; Cronin, L.: Influence of Acceleration on Pulmonary Physiology. Fed. Proc., 22:1024, 1963.